

The Chemical Reactor Design Tool:
A Portable Software Package for Education and Reactor Engineering

by

Brigette Marie Rosendall

A thesis submitted in partial fulfillment
of the requirements for the degree of

Master of Science in Chemical Engineering

University of Washington

1994

Approved by _____
(Chairperson of Supervisory Committee)

Program Authorized
to Offer Degree _____

Date _____

In presenting this thesis in partial fulfillment of the requirements for a Master's degree at the University of Washington, I agree that the Library shall make its copies freely available for inspection. I further agree that extensive copying of this thesis is allowable only for scholarly purposes, consistent with "fair use" as prescribed in the U.S. Copyright Law. Any other reproduction for any purposes or by any means shall not be allowed without my written permission.

Signature _____

Date _____

University of Washington

Abstract

THE CHEMICAL REACTOR DESIGN TOOL:
A PORTABLE SOFTWARE PACKAGE FOR EDUCATION AND REACTION
ENGINEERING

by Brigette M. Rosendall

Chairperson of the Supervisory Committee: Professor Bruce A. Finlayson
Department of Chemical Engineering

The Chemical Reactor Design Tool (CRDT) is a set of computer programs that solves the equations describing common chemical reactor models. The types of reactors that can be modeled include batch reactors, continuous stirred tank reactors, plug flow reactors, plug flow reactors with axial dispersion, and tubular flow reactors with radial dispersion. The models used are similar to those in the common reactor design textbooks. The most general equations describing the particular reactor are used for the base model so that any complexities can be included.

CRDT is composed of three main components. The first is the window driven program that prompts the user for input. This input is required by the second component, the FORTRAN code that solves the mathematical models. The third component is the set of programs that use the output from the FORTRAN programs to generate graphical output.

CRDT can be used as a teaching tool. At the undergraduate level, complicated reactor models often cannot be solved by the student due to the complexity of the mathematics. CRDT allows the student to study such complex models without learning all of the required numerical techniques. Also, CRDT allows the student to compare many

different models in a short amount of time. The effectiveness of using CRDT as a teaching tool is demonstrated with two examples from common reactor design textbooks.

CRDT is also an effective design tool. It can be used to investigate many different phenomenon. The effects of axial and radial dispersion can be easily studied by comparing results of the PFR model with the results of the PFR with axial diffusion model and the two-dimensional model. Heterogeneous effects of catalyst packing can be analyzed by choosing external resistance under the mass transfer resistance menu and providing the appropriate parameters. Heat transfer at the wall can be included for all reactor types. Pressure drop for packed or empty tubes can be modeled. Corresponding changes in velocity and density are automatically taken into account for the gas-phase. Investigating all these effects allows the user to choose an appropriate model for their reaction system. *A priori* criterion can be used to estimate the importance of certain effects, but the predictions are not always accurate. The use of CRDT as a design tool is demonstrated by analyzing three industrial packed-bed reactors. The results are compared to the developed criteria.

TABLE OF CONTENTS

List of Figures	iii
List of Tables	iv
Chapter 1. Introduction	1
Chapter 2. The Models	5
2.1. Batch Reactor	5
2.2. Continuous Stirred Tank Reactor	7
2.3. Plug Flow Reactor	9
2.4. Plug Flow Reactor with Axial Dispersion.	11
2.5. Tubular Flow Reactor with Radial Dispersion (2-D Reactor)	13
2.6. Heterogeneous effects	14
Chapter 3. The Methods	17
3.1. Non-linear Algebraic Equations	17
3.2. The Initial Guess	20
3.3. Ordinary Differential Equations - Initial Value Problems	27
3.4. Ordinary Differential Equations - Boundary Value Problems	28
3.5. Partial Differential Equations	32
Chapter 4. Textbook Examples	37
4.1. Ethylene Glycol Example	37
4.2. N-(2-Hydroxypropyl) Imidazolidinon Example	38
Chapter 5. Criteria	57
5.1. Heterogeneity	57
5.2. Density Variations	58
5.3. Radial Dispersion	59
5.4. Axial Dispersion	61
Chapter 6. Sulfur Trioxide Reactor	62
Chapter 7. Phthalic Anhydride Reactor	71
Chapter 8. Maleic Anhydride Reactor	79
Chapter 9. Conclusions and Recommendations	87

List of References	90
Appendix A. Nomenclature	92
Appendix B. FORTRAN Rate Subroutines	96
B.1. Sulfur Trioxide Reactor	96
B.2. Phthalic Anhydride Reactor	97
B.3. Maleic Anhydride Reactor	98

LIST OF FIGURES

Figure 3.1: Bounds on the Extents of Reaction for the Oxidation of O-Xylene to Phthalic Anhydride	36
Figure 4.1: Case A	52
Figure 4.2: Case B	53
Figure 4.3: Case C	54
Figure 4.4: Case D	55
Figure 4.5: Case E	56
Figure 6.1: Conversion for the Sulfur Trioxide Reactor Comparison	68
Figure 6.2: Temperature Profiles for the Sulfur Trioxide Reactor Comparison	68
Figure 6.3: Convection, Dispersion, and Rate Terms for the Sulfur Trioxide Mass Balance	69
Figure 6.4: Comparison of Conversion for Various Effects in the Sulfur Trioxide Reactor	70
Figure 7.1: Conversion for the Phthalic Anhydride Reactor Comparison	76
Figure 7.2: Selectivity for the Phthalic Anhydride Reactor Comparison	76
Figure 7.3: Temperature Profiles for the Phthalic Anhydride Reactor Comparison	77
Figure 7.4: Temperature Profile in the Phthalic Anhydride 2-D Reactor	77
Figure 7.5: Selectivity Comparison for Various Effects in the Phthalic Anhydride Reactor	78
Figure 8.1: Selectivity for the Maleic Anhydride Reactor Comparison	84
Figure 8.2: Temperature Profiles for the Maleic Anhydride Reactor Comparison	84
Figure 8.3: Comparison of Conversion for Various Effects in the Maleic Anhydride Reactor	85
Figure 8.4: Selectivity Comparison for Various Effects in the Maleic Anhydride Reactor	85
Figure 8.5: Convection, Dispersion, and Rate Terms for the Maleic Anhydride Mass Balance	86

LIST OF TABLES

Table 3.1.--Parameters for the Linear Programming Problem	35
Table 4.1.--Part A) REACSET Procedure for one 400 gallon CSTR	42
Table 4.2.--Part B) REACSET Procedure for two 200 gallon CSTRs in Parallel	43
Table 4.3.--Part C) REACSET Procedure for two 200 gallon CSTRs in Series	43
Table 4.4.--Part D) REACSET Procedure for one 400 gallon PFR	44
Table 4.5.--Part E) REACSET Procedure for twenty 20 gallon CSTRs in Series	45
Table 4.6.--Results of the 5 Simulations	45
Table 4.7.--FORTRAN Subroutine Rate for the Steady-State Assumption Case	46
Table 4.8.--REACSET Procedure for Steady-State Assumption Case	47
Table 4.9.--Output for Steady-State Assumption Case	48
Table 4.10.--FORTRAN Subroutine Rate for the General Case	49
Table 4.11.--REACSET Procedure for the General Case	50
Table 4.12.--Output for General Case	51
Table 6.1.--Simulations	66
Table 6.2.--Parameters for Sulfur Trioxide Reactor	66
Table 6.3.--Criterion Results for the Sulfur Trioxide Reactor	67
Table 6.4.--Importance of Phenomena in Sulfur Trioxide Reactor	67
Table 7.1.--Parameters for Phthalic Anhydride Reactor	75
Table 7.2.--Criterion Results for the Phthalic Anhydride Reactor	75
Table 7.3.--Importance of Phenomena in Phthalic Anhydride Reactor	75
Table 8.1.--Parameters for Simulations	83
Table 8.2.--Criterion Results for the Maleic Anhydride Reactor	83
Table 8.3.--Importance of Phenomena in Maleic Anhydride Reactor	83

Acknowledgments

Financial support for this project was provided by the National Science Foundation and the University of Washington. I wish to thank Dr. Finlayson for allowing me to work with him on this project. I have learned much more from him than what is reflected in this thesis. I feel very lucky to have had the chance to learn from him. I must also thank him for the work he has put into this project; including working on his personal time to make sure this project would be successful.

I must thank Garr Godfrey and Shinhak Lee for their participation in this project. Garr did most of the programming for the X-Window interface. Shinhak finished this work after Garr's graduation. Garr also taught me a lot about programming and showed me how to have fun in Seattle. He was a good friend to me. My group members, Ken Westerberg and Christophe Poulain, also deserve my thanks. Ken taught me how to be a graduate student. Any questions I had, he could answer. Christophe has continually been a great support. He can always make me laugh. I look forward to ongoing work with him.

I must give my deepest gratitude to my fiancé, Kevin Geurts, for his constant love and support. If it weren't for him, I would have not gotten this degree. He deserves more appreciation, love, and respect than I could ever put in words.

My family deserves special thanks. Mom and Dad have been a constant source of motivation. Having them be proud of me means very much to me. Their financial support through my undergraduate career made this possible. I would also like to give special thanks to my Grandma Cushman for always believing in me. My sister Erin has also been a great support. I'd like to thank her especially for that \$5 she gave to me when I needed money, making me promise to do the same for her someday—when I'm rich. I'd also like to thank my brother Eric for being my first teacher.

Lastly, I'd like to thank all the friends I have made in the Department—faculty and students. Because of them, these past few years have been some of the best years of my life. Their advice and support has meant a great deal to me. I hope these friendships will last a lifetime.

Chapter 1. Introduction

The Chemical Reactor Design Tool (CRDT) is a set of computer programs that solve the equations describing common chemical reactor models. The types of reactors that can be modeled include batch reactors, continuous stirred tank reactors (CSTR), plug flow reactors (PFR), plug flow reactors including axial diffusion/dispersion, and tubular flow reactors including radial dispersion (two-dimensional reactor). These models are similar to those found in the common reactor design textbooks (see Froment and Bischoff 1990 and Fogler 1986). The most general equations describing the particular reactor are used for the base model so that any complexities can be included. For example, changes in density due to temperature variations, pressure or volume changes, or mole changes due to reaction can be modeled for all reactor types. The effects of external resistance at the surface of a catalyst can be an added complication for all reactor models also. Chapter 2 of this thesis presents the models used by CRDT.

CRDT is composed of three main components. The first is the window driven program that prompts the user for input. This input is required by the second component, the FORTRAN code that solves the mathematical models. The third component is the set of programs that use the output from the FORTRAN programs to generate graphical output.

The first component is a program written in C language using an X-Window interface. It is called REACSET. All other components of CRDT can be executed from within REACSET or individually. REACSET generates an input file that is read by the appropriate FORTRAN program. (This code was written by Garr Godfrey, Shinhak Lee, and Bruce Finlayson.)

Five separate FORTRAN programs make up the second component of CRDT. The titles of these programs are: REACOL, REACFD, AXIALOC, AXIALFD, and CSTR. (REACOL and REACFD were written by Bruce Finlayson. The AXIALFD, AXIALOC,

and CSTR codes were written by the author.) REACOL uses the orthogonal collocation method along with the choice of three ordinary differential equation solvers to model the two-dimensional reactor. REACOL is also used to solve the PFR and batch reactor models by setting the appropriate parameters in the 2-D model to zero. REACFD is the same as REACOL except it uses the finite-difference method to reduce the partial differential equations describing the 2-D reactor to ordinary differential equations. AXIALOC uses the orthogonal collocation method to reduce the ordinary differential equations describing the PFR with axial diffusion to a set of algebraic equations. AXIALFD uses the finite difference method to solve the same problem. Both use a Newton-Raphson method to solve the algebraic equations, but AXIALOC has the Newton-Raphson method backed up by a homotopy method in case the Newton-Raphson method fails to converge on a solution. The program CSTR uses the Newton-Raphson method backed up by a homotopy method to solve the algebraic equations describing a continuous stirred tank reactor. The methods used to solve the models are presented in chapter 3. All the FORTRAN codes write their output to text file format. This output is converted within REACSET to input read by the plotting routines to generate the graphical output.

The third component is made up of two plotting programs: XPLOT and ALPLOT. These codes are written in a combination of the C and FORTRAN languages. They also use an X-Window interface to draw the output on the computer screen. (The original FORTRAN code was written by Mark Finlayson, Bruce Finlayson, and Doug Frick. Garr Godfrey, Shinhak Lee, and Bruce Finlayson wrote the code to convert these original programs to an X-Window interface using the C programming language.) XPLOT draws the two-dimensional output. ALPLOT draws contour and three-dimensional output. Up to six different plots can be viewed concurrently. The variables that can be viewed include concentrations, moles/molar flow rates, temperature, diffusion terms, convection terms, reaction rates, particle concentrations, and wall fluxes. A detailed description of the format

of all input and output files generated by all components of CRDT can be found in the user's manual (Finlayson, *et al.* 1994).

CRDT can be used as a teaching tool. At the undergraduate level, complicated reactor models often cannot be solved by the student due to the complexity of the mathematics. CRDT allows the student to learn the concepts without having to make all assumptions necessary to reduce the problem to one that is solvable. This allows the student to learn about the different phenomenon without having to perform the tedious math. CRDT also provides visual output. The ability to view the relative magnitudes of convection, diffusion, and rate terms together immediately tell the student which phenomena are important to the design. Three dimensional plots show how significant radial gradients are in the reactor. A hot spot in the reactor is nicely demonstrated with a contour plot of the temperature. Chapter 4 illustrates the effectiveness of CRDT as a teaching tool with two examples from common undergraduate reactor design textbooks.

CRDT is also an effective design tool. It can be used to investigate many different phenomena. The effects of axial and radial dispersion can be easily studied by comparing results of the PFR model with the results of the PFR with axial diffusion model and the two-dimensional model. Heterogeneous effects of catalyst packing can be analyzed by choosing external resistance under the mass transfer resistance menu and providing the appropriate parameters. The particle diffusion problem can be solved using the model for the two-dimensional reactor to determine effectiveness factors due to internal resistance to heat and mass transfer. Heat transfer at the wall can be included for all reactor types. Pressure drop for packed or empty tubes can be modeled and corresponding changes in velocity and density are automatically taken into account for the gas-phase. Concentration, temperature, and velocity can vary with radial location at the inlet for the two-dimensional reactor. Investigating all these effects allows the user to choose an appropriate model for their reaction system. Chapters 6-8 demonstrate the use of CRDT as a design tool by

analyzing industrial packed-bed reactors and comparing the results with criterion developed in chapter 5.

Chapter 2. The Models

CRDT is designed to model five reactor types. These include a batch reactor, a continuous stirred tank reactor (CSTR), a plug flow reactor (PFR), a plug flow reactor including axial dispersion (Axial), and a tubular flow reactor including radial dispersion (2-D). Total concentration need not be assumed constant in any of these models.

Heterogeneous effects of catalyst packing can be included in all reactor types. For the tubular reactors, velocity variations and pressure drop down the reactor length can be included in the model. This chapter will show the details of the models used by CRDT. Notation used in this chapter and throughout the thesis is defined in appendix A.

2.1. Batch Reactor

The model for the batch reactor is derived assuming a perfectly mixed reactor with no mass transfer in or out of the reactor. The mole balance for species j is given in equation (2.1) with initial conditions. The energy balance is given in equation (2.2).

$$\frac{dN_j}{dt} = V_R R_j \quad (2.1)$$

$$N_j(0) = N_{j0}$$

$$\sum_{j=1}^N N_j C_{pj} \frac{dT}{dt} = V_R \sum_{i=1}^M (-\Delta H_{rxn,i}) r_i - UA_w(T - T_w) \quad (2.2)$$

$$T(0) = T_0$$

The rate of consumption or production of species j is defined in equation (2.3).

$$R_j = \sum_{i=1}^M \nu_{ji} r_i \quad (2.3)$$

ν_{ji} = stoichiometric coefficient of species j in reaction i (positive for products, negative for reactants).

r_i = rate expression for reaction i .

The reactor pressure or volume may change for gaseous systems. The reactor pressure or

volume can be found at any time with the ideal gas law. The relations used by CRDT are given in equations (2.4) and (2.5).

$$P = P_0 \frac{N_T}{N_{T0}} \frac{T}{T_0} \quad (2.4)$$

$$V_R = V_{R0} \frac{N_T}{N_{T0}} \frac{T}{T_0} \quad (2.5)$$

$$N_T = \sum_{j=1}^N N_j$$

Note that the number of moles for all species in the reaction system must be provided to calculate the total number of moles at any time. Standard initial values for the total pressure, total concentration, and temperature are also needed. A list of required input is given below.

- 1) number of moles (for every component in reaction system if gaseous).
- 2) initial tank volume, pressure (if gaseous), and temperature (if non-isothermal).
- 3) final time.
- 4) heat capacities for each component if non-isothermal.
- 5) heat transfer coefficient, surface area and surface temperature if there is heat transfer at the wall.
- 6) stoichiometric matrix, heats of reaction or formation, and heat and mass transfer coefficients if there is external resistance at the surface of a catalyst.
- 7) rate expressions in a FORTRAN rate subroutine.

Concentrations or partial pressures are often required to evaluate the rate expressions. For gases, these conversions are made with the ideal gas law shown in equations (2.6) and (2.7).

$$C_j = y_j C_{T0} \frac{T_0}{T} \frac{P}{P_0} \quad (2.6)$$

$$P_j = y_j P \quad (2.7)$$

$$y_j = \frac{N_j}{N_T}$$

For liquids, the volume is assumed constant, and the concentration is simply the number of moles divided by the reactor volume.

The resulting problem is a coupled set of first-order, non-linear, ordinary differential equations; an initial value problem. CRDT gives a choice of three different ordinary differential equation integration routines. These include a second-order Runge-Kutta method, a fourth-order Runge-Kutta method (RKF45, Brankin, *et al.* 1992), or an automatic time-stepping implicit integration routine (LSODE, Hindmarsh 1987). Details of these methods are provided in chapter 3.

2.2. Continuous Stirred Tank Reactor

The CSTR model is derived from a mole balance on species j assuming steady-state operation and perfect mixing. The mole and energy balances are given in equations (2.8) and (2.9).

$$F_j - F_{j0} = V_R R_j \quad (2.8)$$

$$\sum_{j=1}^N F_{j0} C_{pj} (T - T_0) = V_R \sum_{i=1}^M (-\Delta H_{rxn,i}) r_i - UA_w (T - T_w) \quad (2.9)$$

Pressure or volume changes in the CSTR can be modeled with CRDT. Standard initial values for the total pressure, total concentration, and temperature must be provided. With these values, the pressure or volume can be calculated by employing the ideal gas law with equations (2.10) and (2.11).

$$P = P_0 \frac{F_T}{F_{T0}} \frac{T}{T_0} \quad (2.10)$$

$$V_R = V_{R0} \frac{F_T}{F_{T0}} \frac{T}{T_0} \quad (2.11)$$

$$F_T = \sum_{j=1}^N F_j$$

Conversion to concentration or partial pressures for evaluation of the rate expression is accomplished with equations (2.12) and (2.13) for gases.

$$C_j = y_j C_T = \frac{F_j}{F_T} C_{T0} \frac{P}{P_0} \frac{T_0}{T} \quad (2.12)$$

$$P_j = y_j P \quad (2.13)$$

For liquids, molar flow rate is converted to concentration with the volumetric flow rate out of the CSTR.

$$C_j = \frac{F_j}{v} \quad (2.14)$$

Notice that all species in the reaction system must be included in the solution in order to calculate total molar flow rate and mole fractions. Required input to CRDT for the CSTR model is listed below.

- 1) number of tanks in series.
- 2) inlet molar flow rates (for every component in reaction system if gaseous).
- 4) inlet tank volumes, total concentration, pressure (if gaseous), and temperature (if non-isothermal).
- 5) heat capacities for each component if non-isothermal.
- 6) heat transfer coefficient, surface area, and surface temperature if there is heat transfer at the wall.
- 7) stoichiometric matrix and heats of reaction (required for calculation of the initial guess).

8) heat and mass transfer coefficients if there is external resistance at the surface of a catalyst.

9) rate expressions in a FORTRAN rate subroutine.

This model for the CSTR results in a set of coupled, non-linear, algebraic equations. These equations are solved by CRDT using the Newton-Raphson method. If the Newton-Raphson method fails to converge, a homotopy method is used. The initial guess for these methods is provided using a linear programming method. Details of these methods are provided in chapter 3.

2.3. Plug Flow Reactor

The model for the PFR is derived from the steady-state continuity equation for species j and from the steady-state energy balance. These balances assume convective transport dominates over diffusive transport. The energy balance includes the removal of energy at the wall. The velocity is constant across the cross section of the reactor, but can vary in the axial direction. The result is shown in equations (2.15) and (2.16) along with the appropriate inlet conditions.

$$\frac{dF_j}{dV_R} = \rho_B R_j \quad j = 1, \dots, N \quad (2.15)$$

$$\sum_{j=1}^N F_j C_{pj} \frac{dT}{dV_R} = \rho_B \sum_{i=1}^M (-\Delta H_{rxn,i}) r_i - \frac{4U}{d_t} (T - T_w) \quad (2.16)$$

$$\text{Inlet Conditions: } F_j(V_R=0) = F_{j0}, \quad T(V_R=0) = T_0$$

For this model, the total concentration (density) can be assumed constant, or it can vary due to temperature changes, pressure drop, and/or mole changes due to reaction.

When the density varies, the velocity also varies to satisfy the continuity equation.

Therefore, with a constant cross sectional area, the velocity can be calculated at any point with equation (2.17).

$$u = u_0 \frac{\rho_0}{\rho} \quad (2.17)$$

The mass density can be calculated at any point with equation (2.18).

$$\rho = C_T \sum_{j=1}^N y_j MW_j \quad (2.18)$$

The pressure drop for tubular reactors is directly proportional to the velocity for both packed and empty tubes in gaseous systems when using the Ergun or Blasius equations, respectively. Therefore, the pressure drop can be calculated with equation (2.19).

$$\frac{dP}{dz} = \left(\frac{dP}{dz} \right)_0 \frac{u}{u_0} \quad (2.19)$$

Inlet Condition: $P = P_0$ at $z = 0$

The inlet pressure gradient for packed beds is calculated with the Ergun equation (Fogler 1986).

$$\left(\frac{dP}{dz} \right)_0 = -\frac{1-\epsilon}{\epsilon^3} \frac{\rho_0 u_0^2}{d_p} \left[\frac{150(1-\epsilon)}{Re_p} + 1.75 \right] \quad (2.20)$$

For empty tubes and turbulent flow, the inlet pressure gradient is found with the Blasius formula (Bird, *et al.* 1960).

$$\left(\frac{dP}{dz} \right)_0 = -\frac{0.158(\rho_0 u_0)^{0.75} \mu^{0.25}}{d_t^{1.25}} u_0 \quad (2.21)$$

For laminar flow, the pressure drop in an empty tube is given in equation (2.22).

$$\left(\frac{dP}{dz} \right)_0 = -\frac{32\mu u_0}{d_t^2} \quad (2.22)$$

Converting to concentrations or partial pressures for evaluation of the rate expression is done using the same equations given for the CSTR, equations (2.11) and (2.12).

The result of the model is a set of coupled, non-linear, ordinary differential equations; the same result as the batch reactor. These are solved in the same manner as the

batch reactor except that the independent variable is reactor volume instead of time.

Required input for this model is given below.

- 1) molar flow rates (for every component in reaction system if gaseous).
- 2) inlet pressure, temperature, and total concentration.
- 3) inlet velocity or inlet volumetric flow rate and cross-sectional area.
- 4) inlet pressure gradient (if gaseous).
- 5) molecular weights.
- 6) final volume.
- 7) heat capacities for each component if non-isothermal.
- 8) heat transfer coefficient, tube radius, and surface temperature if there is heat transfer.
- 9) stoichiometric matrix and heat and mass transfer coefficients if there is external resistance at the surface of a catalyst.
- 10) rate expressions in a FORTRAN rate subroutine.

2.4. Plug Flow Reactor with Axial Dispersion

Equations (2.23) and (2.24) describe the PFR with axial dispersion.

$$\epsilon D_{ea,j} \frac{d^2 C_j}{dz^2} - \frac{d(uC_j)}{dz} + \rho_B R_j = 0 \quad j = 1, \dots, N \quad (2.23)$$

$$\lambda_{ea} \frac{d^2 T}{dz^2} - u \sum_{j=1}^N C_j C_{pj} \frac{dT}{dz} + \rho_B \sum_{i=1}^M (-\Delta H_{rxn,i}) r_i - \frac{4U}{d_t} (T - T_w) = 0 \quad (2.24)$$

Boundary Conditions at $z = 0$:

$$-\epsilon D_{ea,j} \frac{dC_j}{dz} = u_0 C_{j,0} - u(0) C_j(0)$$

$$-\lambda_{ea} \frac{dT}{dz} = u \sum_{j=1}^N C_j C_{pj} [T_0 - T(0)]$$

$z = L$:

$$\frac{dC_j}{dz} = 0 \quad \frac{dT}{dz} = 0$$

Derivation of these equations is the same as the PFR, except that this model includes diffusive transport in the axial direction. Danckwerts boundary conditions are applied at the inlet (Froment and Bischoff 1990). The total concentration, velocity, and pressure can also vary in this model. The velocity, mass density, and pressure are also calculated using equations (2.17), (2.18), and (2.19) respectively for this model. Inlet pressure gradients can be calculated using the appropriate equation (2.20), (2.21), or (2.22). Note that these equations are solved for concentrations, not molar flow rates. Required input for this model is listed below.

- 1) inlet concentrations (for every component in reaction system if gaseous).
- 2) inlet pressure, temperature, and total concentration.
- 3) inlet velocity or inlet volumetric flow rate and cross-sectional area.
- 4) inlet pressure gradient (if gaseous).
- 5) stoichiometric matrix and heats of reaction.
- 6) effective axial diffusivity and effective axial thermal conductivity (if non-isothermal).
- 7) molecular weights.
- 8) heat capacities for each component if non-isothermal.
- 9) heat transfer coefficient, tube radius, and surface temperature if there is heat transfer at the wall.
- 10) Heat and mass transfer coefficients if there is external resistance at the surface of a catalyst.
- 11) rate expressions in a FORTRAN rate subroutine.

This model results in a coupled set of second-order, non-linear, ordinary differential equations; a boundary value problem. This set of differential equations is reduced to a set

of non-linear algebraic equations with either the orthogonal collocation method or the finite difference method. The Newton-Raphson method is used to solve the non-linear algebraic equations. For the orthogonal collocation method, if the Newton-Raphson method fails, a homotopy method is used. Details of the solution can be found in chapter 3.

2.5. Tubular Flow Reactor with Radial Dispersion (2-D Reactor)

Equations (2.25) and (2.26) show the model for the two-dimensional reactor.

$$\frac{1}{A_c} \frac{\partial F_j}{\partial z} - \frac{\epsilon D_{er,j}}{R^2} \left(\frac{\partial^2 C_j}{\partial r'^2} + \frac{1}{r'} \frac{\partial C_j}{\partial r'} \right) + \rho_B R_j = 0 \quad j = 1, \dots, N \quad (2.25)$$

$$\frac{1}{A_c} \sum_{j=1}^N F_j C_{pj} \frac{\partial T}{\partial z} - \frac{\lambda_{er}}{R^2} \left(\frac{\partial^2 T}{\partial r'^2} + \frac{1}{r'} \frac{\partial T}{\partial r'} \right) + \rho_B \sum_{i=1}^M (-\Delta H_{rxn,i}) r_i = 0 \quad (2.26)$$

Inlet Conditions: $F_j(z=0) = F_{j0}$ $T(z=0) = T_0$

Boundary Conditions at $r' = 0$:

$$\frac{dC_j}{dr'} = 0 \quad \frac{dT}{dr'} = 0$$

$r' = 1$:

$$\frac{\epsilon D_{er,j}}{R} \frac{\partial C_j}{\partial r'} = k_w (C_j - C_{w,j}) \quad j = 1, N$$

$$\frac{\lambda_{er}}{R} \frac{\partial T}{\partial r'} = h_w (T - T_w)$$

This model is derived in the same manner as the PFR also. It includes diffusive transport in the radial direction, but not in the axial direction. Note that the model presented here uses a dimensionless tube radius. This is most convenient for the method of solution. Here, the assumption of plug flow is relaxed. CRDT allows for a radial variation in the velocity. Axial variation in the velocity is also allowed as in the other models. The velocity, mass density, and pressure are calculated at any reactor length using equations (2.17), (2.18), and (2.19) respectively. Inlet pressure gradients can be calculated using the appropriate equation (2.20), (2.21), or (2.22) for this model too.

Again, converting from molar flow rates to concentrations or partial pressures for

evaluation of the rate expression is done using the same equations given for the CSTR, equations (2.11) and (2.12).

The list of required input for the reactor model is given below.

- 1) inlet molar flow rates (for every component in reaction system if gaseous).
- 2) inlet pressure, temperature, and total concentration.
- 3) inlet velocity or inlet volumetric flow rate and cross-sectional area.
- 4) inlet pressure gradient (if gaseous).
- 5) reactor length and tube radius.
- 6) effective radial diffusivities and thermal conductivity.
- 7) molecular weights.
- 8) heat capacities for each component if non-isothermal.
- 9) heat transfer coefficient, tube radius, and surface temperature if there is heat transfer.
- 10) stoichiometric matrix, heats of reaction, and heat and mass transfer coefficients if there is external resistance at the surface of a catalyst.
- 11) rate expressions in FORTRAN rate subroutine.

This model is a coupled set of non-linear, partial differential equations. They are reduced to a coupled set of non-linear, ordinary differential equations using either the orthogonal collocation or finite difference method. Then, the initial value problem can be solved using the same methods as the batch reactor and the PFR. Details of the methods of solution can be found in chapter 3.

2.6. Heterogeneous effects

Heterogeneous effects are due to the presence of catalyst packing. Heterogeneous effects require the reaction rate to be evaluated at the concentrations and temperature at the surface of the catalyst. For mass and heat transfer resistance external to the catalyst, the reaction rates along with the surface concentrations and temperature are determined by

solving the set of algebraic equations below.

$$k_m a(C_j - C_{s,j}) = -\rho_B R_j(C_s, T_s) \quad (2.27)$$

$$h_p a(T - T_s) = -\rho_B \sum_{i=1}^M (\Delta H_{rxn,i}) r_i(C_s, T_s) \quad (2.28)$$

These equations are solved in the same manner as the equations describing the CSTR.

Since these equations must be solved every time the reaction rates need to be evaluated, including external resistance greatly increases the solution time.

For heat and mass transfer resistance internal to the catalyst, effectiveness factors must be calculated prior to the simulation. These effectiveness factors are set in the reaction rate subroutine. CRDT can be used to calculate the value of the effectiveness factor by solving the particle diffusion problem stated in equations (2.29) and (2.30).

$$\epsilon \frac{\partial C_j}{\partial t} = D_e \nabla^2 C_j + R_j \quad (2.29)$$

$$\sum_{j=1}^N C_j C_{pj} \frac{\partial T}{\partial t} = k_e \nabla^2 T + \sum_{i=1}^M (-\Delta H_{rxn,i}) r_i \quad (2.30)$$

The solution method for the particle diffusion problem is the same as the two-dimensional reactor. The model for the two-dimensional reactor is in cylindrical coordinates, but the computer code is generalized for either a planar, cylindrical, or spherical geometry. By integrating these equations to steady-state, the effectiveness factor can be found with the following equation (Finlayson 1980).

$$\eta = \frac{a}{\phi^2} \frac{dC/dr' \big|_{r'=1}}{R(C_s, T_s)} \quad (2.31)$$

The parameters in equation (2.31) are defined below.

$$\left[\frac{dC}{dr} \right]_{r=1} = \text{wall flux}$$

$R(C_s, T_s)$ = rate evaluated at bulk conditions (boundary conditions)

ϕ = Thiele modulus

a = geometry dependent, = 1 planar, = 2 cylindrical, = 3 spherical.

Applications of the models presented in this chapter can be found in chapters 4, 6, 7, and 8.

Chapter 3. The Methods

In this chapter, the solution methods are given for the models presented in chapter 2. Four types of methods are discussed: (1) the solution of non-linear algebraic equations, (2) the solution of ordinary differential equations as initial value problems, (3) the solution of ordinary differential equations as boundary value problems, and (4) the solution of partial differential equations. In many instances, a combination of these methods is required to obtain the solution to the models discussed in chapter 2.

3.1. Non-linear Algebraic Equations

To solve non-linear algebraic equations, CRDT uses the Newton-Raphson method backed up by a homotopy method. The application of these two methods is described using the example set of equations below.

$$\begin{aligned} F_1(x_1, x_2, \dots, x_n) &= 0 \\ F_2(x_1, x_2, \dots, x_n) &= 0 \\ &\vdots \\ F_n(x_1, x_2, \dots, x_n) &= 0 \end{aligned} \tag{3.1}$$

These equations can be represented in vector notation shown in equation (3.2)

$$F(\mathbf{x}) = 0 \tag{3.2}$$

The Newton-Raphson method gives \mathbf{x} at the next iteration, $k+1$, with the following equation.

$$\sum_{j=1}^n A_{ij}^k x_j^{k+1} = \sum_{j=1}^n A_{ij}^k x_j^k - F_i(\mathbf{x}) \tag{3.3}$$

Where the jacobian, A , is defined in equation (3.4).

$$A_{ij} = \frac{\partial F_i}{\partial x_j} \tag{3.4}$$

The Newton-Raphson method has converged when the condition in equation (3.5) has been satisfied.

$$(\mathbf{x}^{k+1} - \mathbf{x}^k) < \text{tolerance} \quad (3.5)$$

One of the advantages of this method is that it converges quadratically; therefore, the error between iterations will approach the tolerance quickly when close to the correct answer. To apply this method, an initial guess must be provided. Convergence of the Newton-Raphson method is greatly influence by the initial guess provided (Finlayson 1980). The program switches to a homotopy method if convergence is not obtained after a set number of iterations.

The homotopy method used by CRDT is a differential arclength homotopy continuation method (Seader 1985). This method is applied to equations (3.2) by defining a Newton homotopy, H , that is linear in a homotopy parameter, t .

$$\mathbf{H}(\mathbf{x}, t) = \mathbf{F}(\mathbf{x}) - (1 - t)\mathbf{F}(\mathbf{x}^0) \quad (3.6)$$

This equation can be converted to an ordinary differential equation as an initial value problem by differentiating with respect to the arclength. The arclength, p , is the path traced by the solution from $t = 0$, the initial guess, to $t = 1$, the solution. The result of the differentiation is show in equation (3.7).

$$\sum_{j=1}^n \frac{\partial H_i}{\partial x_j} \frac{dx_j}{dp} + \frac{\partial H_i}{\partial t} \frac{dt}{dp} = 0 \quad i = 1, n \quad (3.7)$$

The multi-dimensional form of the Pythagorean theorem can be applied because p is the arclength.

$$\sum_{j=1}^n \left(\frac{dx_j}{dp} \right)^2 + \left(\frac{dt}{dp} \right)^2 = 1 \quad (3.8)$$

These equations can be simplified by defining the parameters in equations (3.9) and (3.10).

$$A_{ij} = \frac{\partial H_i}{\partial x_j} \quad i = 1, n ; j = 1, n \quad (3.9)$$

$$\Phi_j = -(A)_{ji}^{-1} \frac{\partial H_i}{\partial t} \quad j = 1, n \quad (3.10)$$

Combination of equations (3.10) and (3.7) simplifies to equation (3.11).

$$\frac{dx_j}{dp} = \Phi \frac{dt}{dp} \quad j = 1, n \quad (3.11)$$

Equation (3.11) combined with equation (3.8) gives equation (3.12).

$$\frac{dt}{dp} = \left[1 + \sum_{j=1}^n \Phi_j^2 \right]^{-\frac{1}{2}} \quad (3.12)$$

Now we can get the value of x at our next step in the homotopy parameter by using a Euler predictor step.

$$\tilde{t}^{k+1} = t^k + \Delta p \frac{dt}{dp} \quad (3.13)$$

$$\tilde{x}_j^{k+1} = x_j^k + \Delta p \frac{dx_j}{dp} \quad j = 1, n \quad (3.14)$$

To reduce the error in the Euler predictor step, the Newton-Raphson method presented above can be used as a corrector step.

$$x_j^{k+1} = \tilde{x}_j^{k+1} - \sum_{j=1}^n (\tilde{A}^{k+1})_{ji}^{-1} H(\tilde{x}^{k+1}) \quad (3.15)$$

The solution to the set of equations is found when $t = 1$. The advantage of this homotopy method is that convergence is readily attained in nearly all cases. A possible convergence difficulty occurs when the jacobian becomes singular during the solution path. This difficulty is remedied by halving the step size of the homotopy parameter and starting the solution over. Another possible remedy would be to choose the independent variable so the jacobian is not singular. In the above method, the independent variable is always the

homotopy parameter. This need not be the case (see Seader 1985). A method for obtaining a suitable initial guess for these two methods is provided in the next section.

3.2. The Initial Guess

Obtaining a reasonable initial guess is problem dependent. The Newton-Raphson method backed up by the homotopy method is used in the solution of the CSTR, external resistance to mass transfer, and the PFR with axial diffusion models. The initial guess is obtained in a similar manner for these problems.

The similarity between these problems is that they are all governed by a chemically reacting system. According to Gavalas (1968), a basic property of chemically reacting systems is that for a closed uniform system, the state variables of that system are bounded. It is known that the concentrations and temperature are bounded between some maximum and minimum values. The concentrations and temperature corresponding to the maximum temperature for exothermic reactions, and the minimum temperature for endothermic reactions, provides a suitable initial guess for the Newton-Raphson and homotopy methods. This was proven by running these methods for a wide range of parameters with the external resistance model. For this wide range of parameters, two initial guesses were chosen, the first corresponding to the bulk conditions and the second corresponding to the concentrations and temperature that maximize temperature for exothermic reactions (minimized temperature for endothermic reactions). It was found that the initial guess corresponding to the maximum (minimum) temperature converged in all cases for the range of parameters tested. Using an initial guess of bulk conditions had convergence difficulties. The Newton-Raphson method experienced many more convergence difficulties than the homotopy method.

It is not necessary to know the rates of reaction to find this maximum temperature change. To demonstrate, consider the equations governing the external resistance problem restated in equations (3.16) and (3.17).

$$k_m a(C_j - C_{s,j}) = -\rho_B \sum_{i=1}^M v_{ij} r_i(C_s, T_s) \quad j = 1, N \quad (3.16)$$

$$h_p a(T_s - T) = \rho_B \sum_{i=1}^M (-\Delta H_{rxn,i}) r_i(C_s, T_s) \quad (3.17)$$

If equations (3.16) are each multiplied by the species individual heat of formation and then summed over $j = 1$ to N , the result shown in equation (3.18) is obtained.

$$\sum_{j=1}^N H_{f,j} k_m a(C_{s,j} - C_j) = -\sum_{j=1}^N H_{f,j} \rho_B \sum_{i=1}^M v_{ij} r_i(C_s, T_s) \quad (3.18)$$

Given the definition of the heat of reaction in equation (3.19), equation (3.18) can be written as in equation (3.20).

$$\Delta H_{rxn,i} = \sum_{j=1}^N v_{ij} H_{f,j} \quad (3.19)$$

$$\sum_{j=1}^N H_{f,j} k_m a(C_{s,j} - C_j) = -\rho_B \sum_{i=1}^M (-\Delta H_{rxn,i}) r_i(C_s, T_s) \quad (3.20)$$

Combining equations (3.17) and (3.20) eliminates the reaction rates to give equation (3.21).

$$h_p a(T_s - T) = -\sum_{j=1}^N H_{f,j} k_m a(C_{s,j} - C_j) \quad (3.21)$$

For convenience, the independent extents of reaction, ξ_j , are defined as in equation (3.22).

$$k_m a(C_j - C_{s,j}) = -\sum_{i=1}^S v_{ij} \xi_i \quad j = 1, N \quad (3.22)$$

Equation (3.23) is the combination of equations (3.21) and (3.22).

$$T_{s,obj} = \frac{\sum_{i=1}^S (-\Delta H_{rxn,i}) \xi_i}{h_{pa}} + T \quad (3.23)$$

Since concentrations cannot be negative, equation (3.22) can be written as equation (3.24).

$$-\sum_{i=1}^S v_{ij} \xi_i \leq k_{ma} C_j \quad \text{for } j = 1, N \quad (3.24)$$

The maximum (minimum) temperature can be found using linear programming methods by using equation (3.23) as the objective function. The extents of reaction are the feasible vector, and equations (3.24) serve as secondary (inequality) constraints with positive extents of reaction being the primary (non-negativity) constraints (Edgar, *et al.* 1988 and Press, *et al.* 1989). Reverse reactions are not accounted for since extents of reactions are used as the non-negativity constraint. The error introduced by assuming the reactions are irreversible is insignificant in obtaining an initial guess since the predicted optimum will still be within the bounds of the reaction system (see figure 3.1). The initial guess may not be the maximum (minimum) temperature for cases where the reactions are reversible but this doesn't limit the final solution of equations (3.16) and (3.17). It is still possible for the Newton-Raphson or homotopy methods to converge to a final solution with a greater (lesser) temperature than the maximum (minimum) initial guess.

In general, the objective function can be represented as equation (3.25) and the primary constraints would be equation (3.26).

$$z = \sum_{i=1}^S a_{oi} x_i + a_{oo} \quad (3.25)$$

$$x_i \geq 0 \quad i = 1, S \quad (3.26)$$

Equation (3.27) gives one type of secondary constraint (the only type necessary for this problem).

$$\sum_{i=1}^S a_{ji}x_i \leq b_j \quad \text{where } b_j \geq 0 \quad \text{for } j = 1, N \quad (3.27)$$

The analysis given above for the external resistance problem can be applied to the CSTR problem to yield similar results. Using the definition for extent of reaction in equation (3.28), the objective function is shown in equation (3.29).

$$F_{j0} - F_j = -\sum_{i=1}^S v_{ij}\xi_i \quad \text{for } j = 1, N \quad (3.28)$$

$$T_{\text{obj}} = \frac{\sum_{i=1}^S (-\Delta H_{\text{rxn},i})\xi_i + \sum_{j=1}^N F_{j0}C_{pj0}T_0 + UaT_w}{\sum_{j=1}^N F_{j0}C_{pj0} + Ua} \quad (3.29)$$

The secondary constraints are shown in equations (3.30).

$$-\sum_{i=1}^S v_{ij}\xi_i \leq F_{j0} \quad \text{for } j = 1, N \quad (3.30)$$

To apply the same analysis to the axial diffusion problem, the equations are written in non-dimensional form and it must be assumed that the Péclet numbers in the mass transfer equations are equal to the Péclet number in the heat transfer equation.

$$\frac{1}{\text{Pe}} \frac{d^2 C_j}{dz^2} - \frac{dC_j}{dz} = -\text{Da}_I \sum_{i=1}^M v_{ij}r_i \quad \text{for } i = 1, N \quad (3.31)$$

$$\frac{1}{\text{Pe}} \frac{d^2 T}{dz^2} - \frac{dT}{dz} = -\beta \text{Da}_I \sum_{i=1}^M (-\Delta H_{\text{rxn},i})r_i \quad (3.32)$$

Corresponding boundary conditions are given below.

$z = 0$:

$$\frac{dC_j}{dz} = Pe(C_j - C_{j0}) \quad \text{for } j = 1, N$$

$$\frac{dT}{dz} = Pe(T - T_0)$$

$z = 1$:

$$\frac{dC_j}{dz} = 0 \quad j = 1, N$$

$$\frac{dT}{dz} = 0$$

If equations (3.31) are multiplied by $\beta H_{f,j}$ and summed over $j = 1$ to N , the result can be combined with equation (3.32) to give equation (3.33).

$$\frac{1}{Pe} \frac{d^2}{dz^2} \left(\sum_{j=1}^N \beta H_{f,j} C_j + T \right) - \frac{d}{dz} \left(\sum_{j=1}^N \beta H_{f,j} C_j + T \right) = 0 \quad (3.33)$$

Performing a similar manipulation to the boundary conditions results in the equations below.

$z = 0$:

$$\frac{d}{dz} \left(\sum_{j=1}^N \beta H_{f,j} C_j + T \right) = Pe \left(\sum_{j=1}^N \beta H_{f,j} C_j + T - \sum_{j=1}^N \beta H_{f,j} C_{j0} - T_0 \right)$$

$z = 1$:

$$\frac{d}{dz} \left(\sum_{j=1}^N \beta H_{f,j} C_j + T \right) = 0$$

The differential equation (3.33) can be solved analytically using the above boundary conditions to give equation (3.34).

$$T = T_0 - \sum_{j=1}^N \beta H_{f,j} (C_j - C_{j0}) \quad (3.34)$$

The extent of reaction for this problem is defined in equation (3.35).

$$C_{j0} - C_j = - \sum_{i=1}^S v_{ij} \xi_i \quad \text{for } j = 1, N \quad (3.35)$$

Combining equations (3.34) and (3.35) with the definition for the heat of reaction gives the objective function.

$$T_{\text{obj}} = \beta \sum_{i=1}^S (-\Delta H_{\text{rxn},i}) \xi_i + T_0 \quad (3.36)$$

The secondary constraints are given in equation (3.37).

$$- \sum_{i=1}^S v_{ij} \xi_i \leq C_{j0} \quad j = 1, N \quad (3.37)$$

Table 1 summarizes the results of the three analyses. The maximum or minimum temperature can be found using the same algorithm for each type of problem. The Simplex method is used to solve this linear programming problem (Edgar, *et al.* 1988 and Press, *et al.* 1989).

Since it is not necessarily known *a priori* whether the reaction system is exothermic or endothermic, the objective function of the linear programming problem is always maximized. The algorithm returns the maximum temperature, z , and the vector, x , which maximizes the objective function. The concentrations corresponding to the maximum temperature are calculated for each case with the equation used to define the extents of reaction.

If the algorithm returns a maximum value of z equal to a_{00} , then it is assumed the reaction system is endothermic. The signs of the heats of reaction are all changed to make the reaction system exothermic overall and the linear programming problem is resolved. Then we know the maximum temperature difference by applying equation (3.38) and the minimum temperature from equation (3.39).

$$\Delta T_{\max} = z - a_{oo} \quad (3.38)$$

$$T_{\min} = a_{oo} - \Delta T_{\max} \quad (3.39)$$

(Note that a_{oo} is not the inlet temperature for a CSTR with heating/cooling but more of an "average" value of the inlet and wall temperatures. Generally, for an endothermic system, the wall temperature is usually slightly greater than or equal to the inlet temperature so any error introduced by using this "average" value is negligible.) The concentrations corresponding to this minimum are calculated from the extents of reaction returned from the algorithm using the appropriate definition.

As an example, take the oxidation of o-xylene to form phthalic anhydride:



For this example, $N = 5$, $M = 3$, and $S = 2$. Let C_1 , C_2 , C_3 , C_4 , and C_5 represent the concentrations of C_8H_{10} , O_2 , $\text{C}_8\text{H}_4\text{O}_3$, H_2O , and CO_2 . For the external resistance problem, equations (3.16) are given below.

$$\begin{aligned} k_m a(C_{s,1} - C_1) &= \rho_B[-r_1 - r_2] \\ k_m a(C_{s,2} - C_2) &= \rho_B\left[-3r_1 - \frac{21}{2}r_2 - \frac{15}{2}r_3\right] \\ k_m a(C_{s,3} - C_3) &= \rho_B[r_1 - r_3] \\ k_m a(C_{s,4} - C_4) &= \rho_B[3r_1 + 5r_2 + 2r_3] \\ k_m a(C_{s,5} - C_5) &= \rho_B[8r_2 + 8r_3] \end{aligned} \quad (3.40)$$

Equation (3.17) is given in equation (3.41).

$$h_p a(T_s - T) = \rho_B[-\Delta H_{\text{rxn},1}r_1 - \Delta H_{\text{rxn},2}r_2 - \Delta H_{\text{rxn},3}r_3] \quad (3.41)$$

The extents of reaction are defined in terms of independent reactions 1 and 2 and are given in equations (3.42).

$$\begin{aligned}
 k_m a(C_{s,1} - C_1) &= \xi_1 + \xi_2 \\
 k_m a(C_{s,2} - C_2) &= 3\xi_1 + \frac{21}{2}\xi_2 \\
 k_m a(C_{s,3} - C_3) &= -\xi_1 \\
 k_m a(C_{s,4} - C_4) &= -3\xi_1 - 5\xi_2 \\
 k_m a(C_{s,5} - C_5) &= -8\xi_2
 \end{aligned}
 \tag{3.42}$$

The objective function is given in equation 3.43.

$$T_s = \frac{-\Delta H_{rxn,1}\xi_1 - \Delta H_{rxn,2}\xi_2}{h_{pa}} + T
 \tag{3.43}$$

The secondary constraints are represented by equations (3.44)

$$\begin{aligned}
 k_m a C_1 &\geq \xi_1 + \xi_2 \\
 k_m a C_2 &\geq 3\xi_1 + \frac{21}{2}\xi_2 \\
 k_m a C_3 &\geq -\xi_1 \\
 k_m a C_4 &\geq -3\xi_1 - 5\xi_2 \\
 k_m a C_5 &\geq -8\xi_2
 \end{aligned}
 \tag{3.44}$$

Figure 3.1 represents the bounds on the extent of reaction graphically. Notice negative values for the extent of reaction are within the bounds set by equations (3.44) but the linear programming problem treats the region where the extents are positive as the feasible solution region because of the non-negativity constraint.

3.3. Ordinary Differential Equations - Initial Value Problems

The solution of the initial value problem can be accomplished with three different methods using CRDT. Two of the methods are common integration packages. The package RKF45 is a Runge-Kutta Fehlberg fourth-fifth order method (Brankin 1992). This explicit method uses a variable step size automatically generated based on a user supplied tolerance. The second method is called LSODE (Hindmarsh 1983). The program

LSODE also has automatic step size control based on a user supplied tolerance, but LSODE is an implicit method. LSODE is the method of choice for stiff problems and for problems where integrating to steady-state. RKF45 is usually more accurate than LSODE, but can also be slower.

For cases where a fixed time step is desired, a second-order Runge-Kutta method, RK2, is an option. For the example differential equation given below, the two-step method is given in equations (3.45) and (3.46).

$$\frac{dy}{dt} = f(y,t) \quad (3.45)$$

$$\tilde{y}^{n+1} = y^n + \Delta t f(y^n, t^n) \quad (3.46)$$

$$y^{n+1} = y^n + \frac{\Delta t}{2} [f(y^n, t^n) + f(\tilde{y}^{n+1}, t^{n+1})] \quad (3.47)$$

The batch reactor, PFR, and two-dimensional reactor all use an ODE-IVP solver. CRDT can be used to solve any ODE-IVP by stating the problem in the form of either the batch reactor or PFR, providing the required input, and choosing the desired method of solution.

3.4. Ordinary Differential Equations - Boundary Value Problems

CRDT uses two different methods for the solution of the boundary value problems, the finite difference method and the orthogonal collocation method. The PFR with axial diffusion is a specific example of a ODE-BVP. A non-dimensional form of the equations describing the PFR with axial diffusion is given in equations (3.48) and (3.49).

$$\frac{1}{Pe_{mL,j}} \frac{d^2 C_j}{dz^2} - \frac{d(uC_j)}{dz} + Da_I R_j = 0 \quad \text{for } j = 1, N \quad (3.48)$$

$$\frac{1}{Pe_{h,L}} \frac{d^2 T}{dz^2} - \left(\sum_{j=1}^N C_{pj} C_j \right) u \frac{dT}{dz} + Da_{III} RT - Bi(T - T_w) = 0 \quad (3.49)$$

The boundary conditions are given below.

$z = 0$:

$$\frac{dC_j}{dz} = uPe_{mL,j}(C_j - C_{j0})$$

$$\frac{dT}{dz} = \left(\sum_{j=1}^N C_{pj}C_j \right) uPe_{hL}(T - T_0)$$

$z = 1$:

$$\frac{dC_j}{dz} = 0$$

$$\frac{dT}{dz} = 0$$

In the finite difference method, the domain is divided into a grid of equal Δz . At each of these grid points, a corresponding value of the dependent variables exists. The values of the dependent variables at the grid points are determined with difference formulas. The difference formulas are derived with Taylor series expansions. (Finlayson 1980). Centered difference formulas are applied in this model. The domain is divided from point $k = 1$ to point $k = np$. A false boundary point, $k = 1$, is used at the inlet in this method. The inlet, $z = 0$, corresponds to point $k = 2$. The finite difference formulation for the false point, $k = 1$, is given in equations (3.50) and (3.51).

$$\frac{2(C_{2,j} - C_{1,j})}{Pe_{mL,j}\Delta z^2} + \frac{C_{2,j}(u_3 - u_1)}{2\Delta z} - (C_{2,j} - C_{j0}) \left[\frac{2u_2}{\Delta z} - Pe_{mL,j}u_2^2 \right] - Da_I R_{2,j} = 0 \quad \text{for } j = 1, N \quad (3.50)$$

$$\frac{2(T_2 - T_1)}{Pe_{hL}\Delta z^2} - (T_2 - T_0) \left[\frac{2 \left(\sum_{j=1}^N C_{p2,j}C_{2,j} \right) u_2}{\Delta z} - Pe_{hL} \left(\sum_{j=1}^N C_{p2,j}C_{2,j} \right)^2 u_2^2 \right] - Da_{III} RT_2 + Bi(T_2 - T_w) = 0 \quad (3.51)$$

The finite difference formulation for points $k = 2$ to $k = np-1$ are given in equations (3.52) and (3.53).

$$\begin{aligned} \frac{C_{k+1,j} - 2C_{k,j} + C_{k-1,j}}{Pe_{mL,j}\Delta z^2} - u_k \frac{C_{k+1,j} - C_{k-1,j}}{2\Delta z} \\ - C_{k,j} \frac{u_{k+1} - u_{k-1}}{2\Delta z} + Da_I R_{k,j} = 0 \quad \text{for } j = 1, N \end{aligned} \quad (3.51)$$

$$\begin{aligned} \frac{T_{k+1} - 2T_k + T_{k-1}}{Pe_{h,L}\Delta z^2} - u_k \left(\sum_{j=1}^N C_{pk,j} C_{k,j} \right) \frac{T_{k+1} - T_{k-1}}{2\Delta z} \\ + Da_{III} R T_k - Bi(T_k - T_w) = 0 \end{aligned} \quad (3.52)$$

Originally, a false point was also applied at the exit. Solutions demonstrated oscillations near the exit with this method. A more appropriate method of solution at the boundary is with the finite element method. The advantage of applying the finite element method is the ability to easily handle the natural boundary condition (Finlayson 1992). The finite element equations at point $k = np$ are given in equations (3.53) and (3.54).

$$\begin{aligned} \frac{C_{np-1,j} - C_{np,j}}{Pe_{mL,j}\Delta z^2} + \frac{2u_{np-1}C_{np-1,j} + u_{np}C_{np-1,j} + u_{np-1}C_{np,j} - 4u_{np}C_{np,j}}{6\Delta z} \\ + \frac{1}{6}Da_I R_{np-1,j} + \frac{1}{3}Da_I R_{np,j} = 0 \quad \text{for } j = 1, N \end{aligned} \quad (3.53)$$

$$\begin{aligned} \frac{T_{np-1} - T_{np}}{Pe_{h,L}\Delta z^2} + [u_{np} + u_{np-1}] \left(\sum_{j=1}^N (C_p)_{np-1,j} C_{np-1,j} \right) \frac{T_{np-1} - T_{np}}{12\Delta z} \\ + [3u_{np} + u_{np-1}] \left(\sum_{j=1}^N (C_p)_{np,j} C_{np,j} \right) \frac{T_{np-1} - T_{np}}{12\Delta z} \\ + \frac{1}{6}Da_{III} R T_{np-1} + \frac{1}{3}Da_{III} R T_{np} \\ - \frac{Bi}{6}(T_{np-1} + 2T_{np} - 3T_w) = 0 \end{aligned} \quad (3.54)$$

After applying the finite difference method, the set of $N+1$ ordinary differential equations become a set of $np(N+1)$ non-linear algebraic equations. Note, however, that

there are $np(N+2)$ unknowns (including velocity). The additional equations required for the solution are from continuity, equation (2.17). CRDT solves for the $np(N+1)$ unknown concentrations and temperature with the Newton-Raphson method. The velocities for the current iteration of the Newton-Raphson method are from the previous iteration; they are calculated with equation (2.17) using the current concentrations and temperature. Thus, the solution method for the algebraic equations is actually a successive substitution method.

The second method of solution for boundary value problems is with orthogonal collocation. The orthogonal collocation method provides a much more accurate solution than the finite difference method while using fewer grid points (Finlayson 1980). With this method, the unknowns are expanded in trial functions. These trial functions are a series of orthogonal polynomials. The roots of one of the polynomials are used as the grid points. In this method, the first and second derivatives at any point can be written in terms of the value for the dependent variable at any point as shown in equations (3.55) and (3.56).

$$\left[\frac{dx}{dy} \right]_i = \sum_{k=1}^{np} A_{i,k} x_k \quad (3.55)$$

$$\left[\frac{d^2x}{dy^2} \right]_i = \sum_{k=1}^{np} B_{i,k} x_k \quad (3.56)$$

The values for the **A** and **B** matrices can be found in Finlayson (1980). Applying this method to the boundary condition at the inlet gives the equation at collocation point $i=1$.

$$\sum_{k=1}^{np} A_{1,k} C_{k,j} - u_1 Pe_{mL,j} (C_{1,j} - C_{j0}) = 0 \quad \text{for } j = 1, N \quad (3.57)$$

$$\sum_{k=1}^{np} A_{1,k} T_k - u_1 \left(\sum_{j=1}^N (C_p)_{1,j} C_{1,j} \right) Pe_{hL} (T_1 - T_0) = 0 \quad (3.58)$$

Substituting the definitions in equation (3.55) and (3.56) into the differential equations gives the equations for collocation points $i = 2$ to $np-1$.

$$\left[\frac{1}{Pe_{mL,j}} \sum_{k=1}^{np} B_{i,k} - u_i \sum_{k=1}^{np} A_{i,k} \right] C_{k,j} - C_{i,j} \sum_{k=1}^{np} A_{i,k} u_k + Da_j R_{i,j} = 0 \quad \text{for } j = 1, N \quad (3.59)$$

$$\left[\frac{1}{Pe_{hL}} \sum_{k=1}^{np} B_{i,k} - u_i \left(\sum_{j=1}^N (C_p)_{i,j} C_{i,j} \right) \sum_{k=1}^{np} A_{i,k} \right] T_k + Da_{III} RT_i - Bi(T_i - T_w) = 0 \quad (3.60)$$

Finally, the equations for the boundary condition at the outlet, $i = np$, are shown in equations (3.61) and (3.62).

$$\sum_{k=1}^{np} A_{np,k} C_{k,j} = 0 \quad \text{for } j = 1, N \quad (3.61)$$

$$\sum_{k=1}^{np} A_{np,k} T_k = 0 \quad (3.62)$$

This method also reduces the set of $N+1$ ODEs to a set of $np(N+1)$ non-linear algebraic equations. Again, there are $np(N+2)$ unknowns. The method of solution here is similar to the finite difference method. The difference between the solution here and in the finite difference method is the form of the jacobian. The jacobian in the finite difference method is block tri-diagonal, therefore, a special decomposition can be done. The jacobian for the orthogonal collocation method is dense. The decomposition of the block tri-diagonal matrix is much more efficient than the LU decomposition performed on the dense matrix (Finlayson, 1980). The only other difference between the solution of the orthogonal collocation method and the finite difference method is that the orthogonal collocation method is backed up with the homotopy method.

3.5. Partial Differential Equations

The two-dimensional reactor and the particle diffusion models result in partial differential equations. The orthogonal collocation and finite difference methods are also used to solve these problems. The example partial differential equation shown in equation

(3.63) is the general form of these models. The parameter a is geometry dependent; it is equal to 1 for planar geometry, 2 for cylindrical geometry, and 3 for spherical geometry.

This equation is used demonstrate how these methods are applied.

$$a_1 \frac{\partial C}{\partial z} = a_2 \left(\frac{\partial^2 C}{\partial r^2} + \frac{a-1}{r} \frac{\partial C}{\partial r} \right) + a_3 f(C) = 0 \quad (3.63)$$

Initial Condition: $0 \leq r \leq 1$:

$$C(z=0) = a_4$$

Boundary Conditions: $0 \leq z \leq 1$:

$$r=0: \frac{\partial C}{\partial r} = 0$$

$$r=1: \frac{\partial C}{\partial r} = a_5(C - a_6)$$

Applying the finite difference method (described in the previous section) to this equation gives a set of ordinary differential equations as initial value problems. The grid is divided into (nt) equal intervals. For the node points $i = 1$ to $(nt-1)$, equations (3.64) apply.

$$a_1 \frac{dC_i}{dz} = a_2 \left(\frac{C_{i+1} - 2C_i + C_{i-1}}{\Delta r^2} + \frac{a-1}{r} \frac{C_{i+1} - C_{i-1}}{2\Delta r} \right) + a_3 f(C_i) = 0 \quad (3.64)$$

The boundary conditions applied at $i = 1$ and $i = nt-1$ provide algebraic relations for the boundary points. Points $i = 0$ and $i = nt$ are false points.

$$\frac{C_2 - C_0}{2\Delta r} = 0$$

$$- \frac{C_{np} - C_{np-2}}{2\Delta r} = a_5(C_{np-1} - a_6)$$

The initial condition applies throughout the domain.

$$C_i(z=0) = a_4 \quad \text{for } i = 0, nt$$

The orthogonal collocation method applied to equation (3.63) also results in a set of ordinary differential equations as initial value problems. The following equation is valid for points $i = 2$ to $(np-1)$.

$$a_1 \frac{dC_i}{dz} = a_2 \sum_{k=1}^{np} B_{i,k} C_k + a_3 f(C_i) = 0 \quad (3.64)$$

The equations at points $i = 1$ and $i = np$ are given below.

$$\sum_{k=1}^{np} A_{1,k} C_k = 0$$

$$-\sum_{k=1}^{np} A_{np,k} C_k = a_5 (C_{np} - a_6)$$

The same initial condition applies throughout this domain also.

$$C_i(z=0) = a_4 \quad \text{for } i = 1, nt$$

For both methods, the initial value problem is solved with LSODE, RKF45, or RK2. These methods are described in section 2.1.

As stated in the introduction, a combination of these methods may be needed to solve the model. The CSTR model only needs to solve algebraic equations, usually non-linear. Recall from chapter 2 that any of the reactor models can include external resistance to heat and mass transfer at the surface of a catalyst. When this is the case, the problems include solving a set of algebraic equations along with the original problem. The algebraic equations need to be solved every time the value of the reaction rate is needed. Thus, the more complicated the model, the longer the solution time required.

Table 3.1.--Parameters for the Linear Programming Problem

Parameter	CSTR	External Resistance	Axial Diffusion
z	T_{obj}	T_{obj}	T_{obj}
x_j	ξ_i	ξ_i	ξ_i
a_{00}	$\frac{\sum_{j=1}^N F_{j0} C_{pj0} T_0 + Ua T_w}{\sum_{j=1}^N F_{j0} C_{pj0} + Ua}$	T	T_0
a_{oi}	$\frac{\Delta H_{rxn,i}}{\sum_{j=1}^N F_{j0} C_{pj0} + Ua}$	$\frac{\Delta H_{rxn,i}}{h_p a}$	$\beta \Delta H_{rxn,i}$
a_{ji}	$-v_{ij}$	$-v_{ij}$	$-v_{ij}$
b_j	F_{j0}	$k_m a C_j$	C_{j0}

Chapter 4. Textbook Examples

In this chapter, textbook examples solved using CRDT are presented. These examples demonstrate the effectiveness of CRDT as a teaching tool. The first example is taken from an undergraduate reactor design textbook. It shows how CRDT can be used to analyze the differences between placing CSTRs in series and in parallel. It also demonstrates that when many CSTRs are placed in series, the resulting conversion approaches the conversion of a PFR. The second example is taken from another undergraduate reactor design textbook. This example shows the effects of making assumptions to simplify a problem.

4.1. Ethylene Glycol Example

The first example is taken from Example 4-2, page 117, of H.S. Fogler's Elements of Chemical Reaction Engineering, first edition, Prentice-Hall, Inc., 1986. The reaction is the hydration of ethylene oxide to form ethylene glycol with H_2SO_4 as a catalyst. The reaction and rate expression are given below.



$$R_a = -0.311C_a \quad [=] \quad \frac{\text{lbmol}}{\text{ft}^3\text{min}} \quad (4.1)$$

CRDT is used to compare outlet concentrations and molar flow rates of one 400 gallon (53.47 ft^3) CSTR (part A) with two 200 gallon CSTRs in parallel (part B) and in series (part C). The example is extended to compute concentration profiles for a 400 gallon plug flow reactor (part D) and 20 CSTRs in series with a total volume of 400 gallons (part E). The total inlet flow rate is $3.84 \text{ ft}^3/\text{min}$ and the inlet concentration of ethylene oxide is $4 \text{ lbmol}/\text{ft}^3$ giving an inlet molar flow rate of $15.36 \text{ lbmol}/\text{min}$.

The 400 gallon CSTR and the two CSTRs in parallel should give the same solution. The CSTRs in series should convert more of the ethylene oxide than the CSTRs in parallel. Finally, the PFR will convert the most ethylene oxide of all reactors compared. The 20

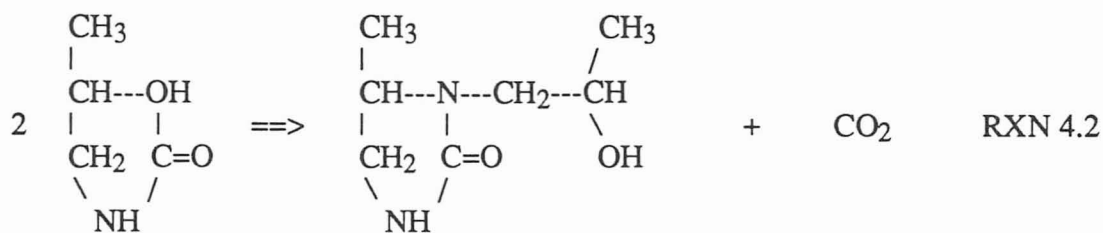
CSTRs will demonstrate the approach of infinite CSTRs in series to PFR behavior.

The procedure for using CRDT for part A through E is presented in tables 4.1 through 4.5, respectively. Plots of the molar flow rate of ethylene oxide versus tanks are presented in figures 4.1, 4.2, 4.3, and 4.5 for parts A, B, C, and E respectively. A plot of molar flow rate versus reactor volume is presented in figure 4.4 for part D. Table 4.6 summarizes the results of the 5 simulations by giving outlet molar flow rates and conversions of ethylene oxide.

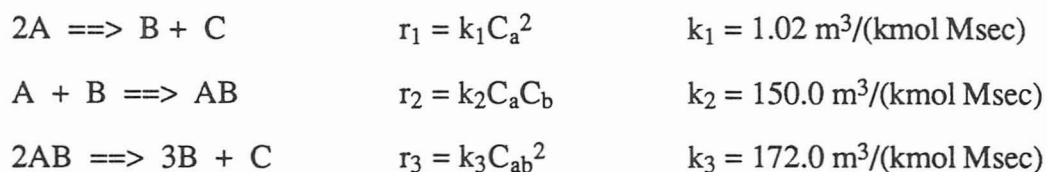
As can be seen in the conversion and in the graphs of the solution, the 400 gallon CSTR and two CSTRs in parallel did give the same solution; the outlet molar flow rate for one of the CSTRs in parallel is exactly half of the single CSTR. The two CSTRs in series convert more of the ethylene oxide than the two in parallel. The PFR gives the highest conversion and comparison of figures 4.4 and 4.5 demonstrates that 20 CSTRs in series do approach the conversion of a PFR.

4.2. N-(2-Hydroxypropyl) Imidazolidinon Example

The second example is taken from Illustration 9.5, page 339, of C.G. Hill's An Introduction to Chemical Engineering Kinetics and Reactor Design, 1st ed., John Wiley & Sons Inc., 1977. The reaction studied is the conversion of 5-methyl-2-oxazolidinone (A) to form N-(2-hydroxypropyl) imidazolidinone (B) and carbon dioxide (C).



The proposed mechanism is given below.



The reaction rates for each species are given in equation (4.3).

$$\begin{aligned}R_a &= -2r_1 - r_2 \\R_b &= r_1 - r_2 + 3r_3 \\R_c &= r_1 + r_3 \\R_{ab} &= r_2 - 2r_3\end{aligned}\tag{4.3}$$

Assuming that at steady state the amount of component AB is constant, then the reaction rate of this component is zero and the simplification in equation (4.4) can be made.

$$\begin{aligned}r_2 &= 2r_3 \\k_2 C_a C_b &= 2k_3 C_{ab}^2\end{aligned}\tag{4.4}$$

The reaction rates in equation (4.3) can be simplified to equation (4.5).

$$\begin{aligned}R_a &= -2r_1 - r_2 \\R_b &= r_1 + \frac{1}{2}r_2 \\R_c &= r_1 + \frac{1}{2}r_2\end{aligned}\tag{4.5}$$

The reaction rates above can be simplified further. For a constant volume system, the concentration of the product can be written in terms of the conversion of the reactant. This simplification is shown in equation (4.6).

$$C_b = \frac{1}{2}(C_{a0} - C_a)\tag{4.6}$$

Then, only the reaction rate of component A needs to be considered. The resulting reaction rate, R_a , is shown in equation (4.7).

$$R_a = -2r_1 - r_2 = -2k_1 C_a^2 - \frac{1}{2}k_2 C_a (C_{a0} - C_a)\tag{4.7}$$

Conversion of species A is defined in equation (4.8).

$$f_a = \frac{C_{a0} - C_a}{C_{a0}}\tag{4.8}$$

With this definition, the rate expression for the steady-state assumption is given below.

$$R_a = -2k_1 C_{a0}^2 (1 - f_a)^2 - \frac{1}{2} k_2 C_{a0}^2 f_a (1 - f_a) \quad (4.9)$$

The conversion resulting in the maximum rate of reaction can be found by differentiating the rate expression with respect to the conversion to give equation (4.10).

$$\frac{dR_a}{df_a} = -4k_1 C_{a0}^2 (1 - f_a) - \frac{1}{2} k_2 C_{a0}^2 (1 - 2f_a) = 0$$

$$f_a = \frac{8k_1 - k_2}{8k_1 - 2k_2} = 0.486 \quad (4.10)$$

To determine the maximum rate of reaction, an inlet concentration is needed. The concentration is calculated in equation (4.11) using the ideal gas law.

$$C_{a0} = \frac{P}{RT} = \frac{1 \text{ bar}}{0.08314 \text{ m}^3 \text{ bar}/(\text{kmol K}) 473 \text{ K}} = 0.025 \text{ kmol/m}^3 \quad (4.11)$$

Then the maximum rate is $|R_{a,\max}| = 0.01205 \text{ kmol/m}^3 \text{ Msec}$. The residence time of a CSTR operating at this maximum rate is given in equation (4.12).

$$\tau = \frac{V_R}{v_0} = \frac{C_{a0} f_a}{-R_a} = \frac{(0.025)(0.486)}{(0.01205)} = 1.0086 \text{ Msec} \quad (4.12)$$

For a 5 liter reactor, the corresponding volumetric flow rate and molar flow rate is given below.

$$v_0 = 0.004957 \text{ m}^3/\text{Msec} \quad (4.13)$$

$$F_{a0} = 0.000124 \text{ Kmol/Msec} \quad (4.14)$$

These results can be verified with CRDT with the rate subroutine in table 4.7. The REACSET procedure is given in table 4.8. The output file is given in table 4.9. CRDT predicts an output concentration of $C_a = 0.01285 \text{ kmol/m}^3$, which correspond to a conversion given below.

$$f_a = \frac{0.025 - 0.0128491}{0.025} = 0.486 \quad (4.15)$$

Thus, the solution found by CRDT is the conversion resulting in the maximum reaction rate

as expected.

Note that CRDT found a physically impossible second solution of $C_a = 0.02644$ kmol/m³. There cannot be more component A than the initial concentration unless the initial concentration of B and C are not zero and the reverse reaction occurs.

CRDT can be used with the general rate expressions in equation (4.3) to test if the steady state assumption is an accurate representation of the proposed mechanism. The rate subroutine for this case is in table 4.10. The REACSET procedure is shown in table 4.11. The output file is given in table 4.12. Using the same reactor specifications, CRDT predicts an output concentration of $C_a = 0.023358$ kmol/m³ corresponding to a conversion of $f_a = 0.06568$.

This result is much different from the result found using the steady state assumption. This proves the assumption is not valid. This example demonstrates how a commonly used approximation can yield inaccurate results. The parameters used with the steady state assumption predict nearly 50% conversion while under the same conditions, using the complete mechanism results in a conversion of less than 10%. Not only is the conversion less than expected, but the reactor would not be operating at the optimum capacity. A much longer residence time than predicted using the steady state assumption is required to operate the reactor at the maximum reaction rate.

The two examples presented above demonstrate how effective CRDT can be as a teaching tool. The first example shows how reactor design principles can be demonstrated simply and visually with CRDT and its graphical output. The second example demonstrates that assumptions need not be made when using CRDT. The set up for the steady-state assumption takes more time than solving the problem using the entire reaction system with CRDT.

Table 4.1.--Part A) REACSET Procedure for one 400 gallon CSTR

Menu 1, File: New

Menu 2, Reactor:

2a: Reactor Type: CSTR with 1 reactor in series.

2b: Mass Transfer Resistance: Homogeneous

2c: Reaction Rates:

- # Chemical components to specify parameters for = 1.
- Total # of components, reactions and stoichiometric matrix not needed since isothermal with no parameters required.
- Liquid phase, volume constant.
- Temperature, isothermal, no parameters required.

2d: Specs (Dimensional): Set tank volumes = 53.47

Menu 3, Equation:

3d: Inlet Conditions:

Component 1 molar flow rate = 15.36

Set total inlet concentration = 4

Menu 4, Run:

4a: View Input File. Shows input.dat

4b: Select Plots: choose Component 1 moles

4c: Run:

- Input file = input.dat
- Program = cstr
- Output file = cstrex4_2a.out

4d: View Output File: Can view cstrex4_2a.out

4e: View Plots: Graphs outlet concentration or molar flow rate verses reactor number.

Table 4.2.--Part B) REACSET Procedure for two 200 gallon CSTRs in Parallel

Menu settings are same as Part A, except:

2d: Specs (Dimensional): Tank volume changed to 26.735 instead of 53.47

3d: Inlet Conditions: Molar flow rate changed to 7.86

4c: Run: Change output file name to cstrex4_2b.out

Table 4.3.--Part C) REACSET Procedure for two 200 gallon CSTRs in Series

Menu setting are same as Part A, except:

2a: Reactor Type: Change number of reactors in series to 2.

2d: Specs (Dimensional): Set two reactor volumes to 26.735

4c: Run: Change output file name to cstrex4_2c.out

Table 4.4.--Part D) REACSET Procedure for one 400 gallon PFR

Menu setting are same as Part A, except:

2a: Reactor Type: PFR.

2d: Specs (Dimensional):

- radius = 1.1256 (L/D = 6)

Menu 3, Equation:

3a: Axial/Time Integration:

- Can choose any of the three integration routines. (RKF45 with default values).

- Printing: 10 printing times, equal intervals.

- Integrate to: Reactor volume, 53.47

3d: Inlet Conditions:

- Flow rate chosen instead of velocity since provided.

- Cross Sectional Area = 3.98 (L/D = 6).

- Inlet Conditions: Component 1 = 15.36

Total Concentration = 4

Flow Rate = 3.84

Menu 4, Run:

4b: Select Plots: Select moles: Component 1.

4c: Run:

- Input file = input.dat

- Program = reacol

- Output file = pfrex4_2d.out

4e: View Plots: Graphs concentration or molar flow rate vs. volume.

Table 4.5.--Part E) REACSET Procedure for twenty 20 gallon CSTRs in Series

Menu setting are same as Part C, except:

2a: Reactor Type: Change number of reactors in series to 20

2d: Specs (Dimensional): Set reactor volumes to 2.6735

Table 4.6.--Results of the 5 Simulations

Part	Molar Flow Rate	Conversion
A	2.88	0.81
B	1.44	0.81
C Reactor 1	4.85	0.68
Reactor 2	1.53	0.90
D	0.20	0.987
E	0.30	0.980

Table 4.7.--FORTRAN Subroutine Rate for the Steady-State Assumption Case

```
subroutine rate(kon,c,ra,eta,t,rt,etat)
implicit double precision (a-h,o-z)
dimension c(21),eta(21),ra(21),par(8)
common /tosave/ par
go to (5,20), kon
5  continue
   return
20  continue
   rk1 = 1.02
   rk2 = 150.0
   cao = 0.025
   eta(1) = 1.
   r1 = rk1*c(1)**2
   r2 = rk2*c(1)*0.5*(cao - c(1))
   ra(1) = -2.0*r1 - r2
   etat = 0.0
   rt = 0.0
   return
end
```

Table 4.8.--REACSET Procedure for Steady-State Assumption Case

Menu 1, File: New

Menu 2, Reactor:

2a: Reactor Type: CSTR with 1 reactor in series.

2b: Mass Transfer Resistance: Homogeneous

2c: Reaction Rates:

- # Chemical components to specify parameters for = 1.
- Total # of components, reactions and stoichiometric matrix not needed since isothermal with no parameters required.
- Liquid phase, volume constant.
- Temperature, isothermal, no parameters required.

2d: Specs (Dimensional): Set tank volumes = 0.005

Menu 3, Equation:

3d: Inlet Conditions:

Component 1 molar flow rate = 0.000124

Set total inlet concentration = 0.025

Menu 4, Run:

4a: View Input File. Shows input.dat

4c: Run:

- Input file = input.dat
- Program = cstr
- Output file = output.dat

4d: View Output File: View output.dat

Table 4.9.--Output for Steady-State Assumption Case

This program calculates outlet molar flow rates for 1 components
for 1 tank(s).

The phase is liquid

The standard initial values are:

Total concentration = 0.2500E-01

Pressure = 0.0000E+00

Temperature = 0.0000E+00

The reaction system is isothermal

The Da 1 = 0.1000E+01

The volume of tank 1 = 0.5000E-02

The inlet molar flow rates for tank 1:

Component 1 = 0.1239E-03

MULTIPLE STEADY STATES

One solution:

For CSTR number 1

Molar flow rates:

Component 1 = 6.36879E-05

Concentrations:

Component 1 = 1.28486E-02

Volumetric Flow Rate = 4.95680E-03

Another solution:

For CSTR number 1

Molar flow rates:

Component 1 = 1.31049E-04

Concentrations:

Component 1 = 2.64381E-02

Volumetric Flow Rate = 4.95680E-03

Table 4.10.--FORTRAN Subroutine Rate for the General Case

```
subroutine rate(kon,c,ra,eta,t,rt,etat)
implicit double precision (a-h,o-z)
dimension c(21),eta(21),ra(21),par(8)
common /tosave/ par
go to (5,20), kon
5  continue
   return
20  continue
   rk1 = 1.02
   rk2 = 150.0
   rk3 = 172.0
   eta(1) = 1.
   eta(2) = 1.
   eta(3) = 1.
   eta(4) = 1.
   r1 = rk1*c(1)**2
   r2 = rk2*c(1)*c(2)
   r3 = rk3*c(4)**2
   ra(1) = -2.0*r1 - r2
   ra(2) = r1 - r2 + 3.0*r3
   ra(3) = r1 + r3
   ra(4) = r2 - 2.0*r3
   etat = 0.0
   rt = 0.0
   return
end
```

Table 4.11.--REACSET Procedure for the General Case

Menu setting are same as table 4.8, except:

2c: Reaction Rates:

- # Chemical components to specify parameters for = 4.

3d: Inlet Conditions:

Component 1 molar flow rate = 0.000124

Component 2-4 molar flow rate = 0

Table 4.12.--Output for General Case

This program calculates outlet molar flow rates for 4 components for 1 tank(s).

The phase is liquid

The standard initial values are:

Total concentration = 0.2500E-01

Pressure = 0.1000E+01

Temperature = 0.1000E+01

The reaction system is isothermal

The Da 1 = 0.1000E+01

The Da 2 = 0.1000E+01

The Da 3 = 0.1000E+01

The Da 4 = 0.1000E+01

The volume of tank 1 = 0.5000E-02

The inlet molar flow rates for tank 1:

Component 1 = 0.1239E-03

Component 2 = 0.0000E+00

Component 3 = 0.0000E+00

Component 4 = 0.0000E+00

For CSTR number 1

Molar flow rates:

Component 1 = 1.15780E-04

Component 2 = 7.28586E-07

Component 3 = 2.95618E-06

Component 4 = 2.22760E-06

Concentrations:

Component 1 = 2.33578E-02

Component 2 = 1.46987E-04

Component 3 = 5.96390E-04

Component 4 = 4.49403E-04

Volumetric Flow Rate = 4.95680E-03

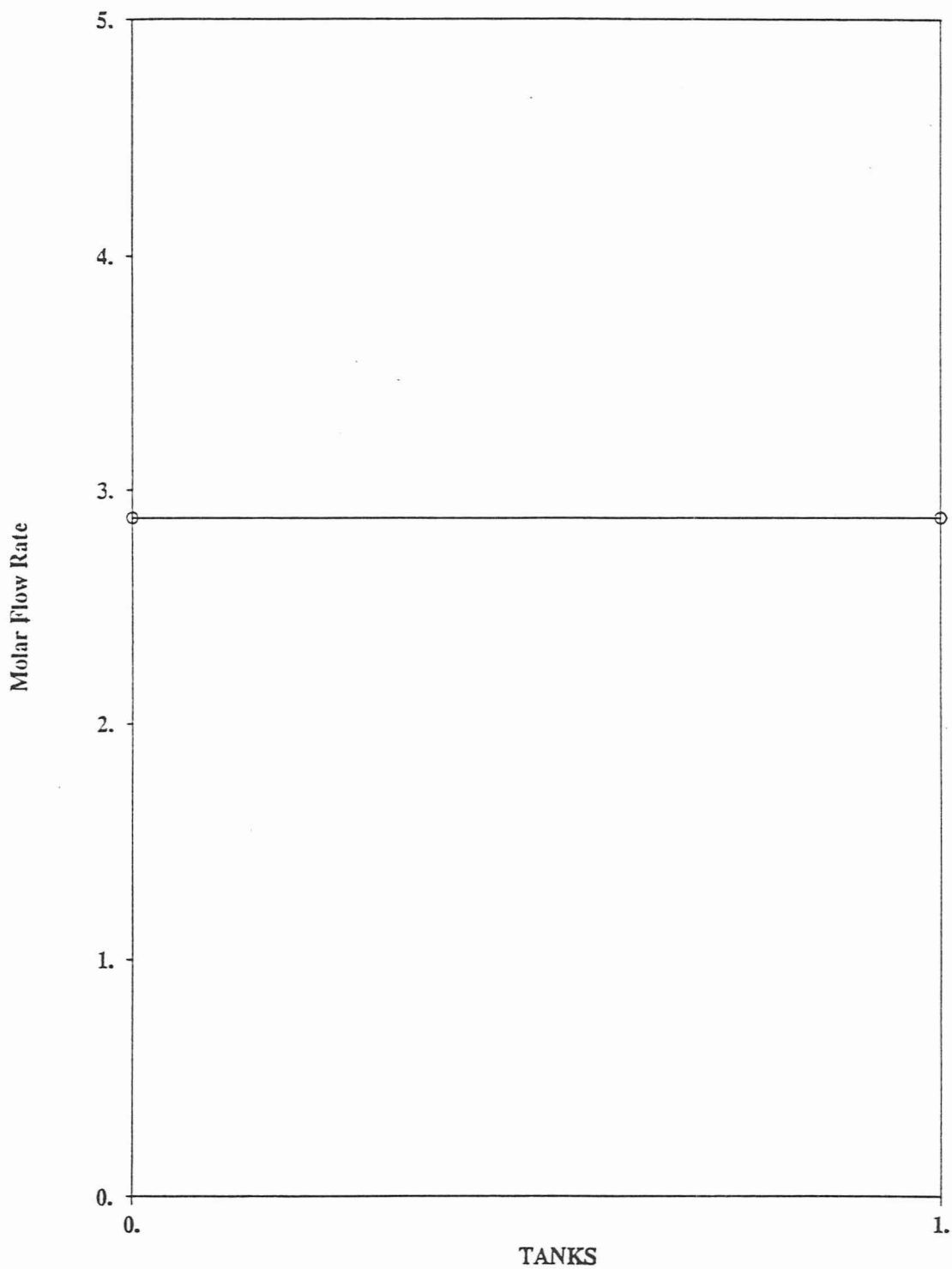


Figure 4.1: Case A

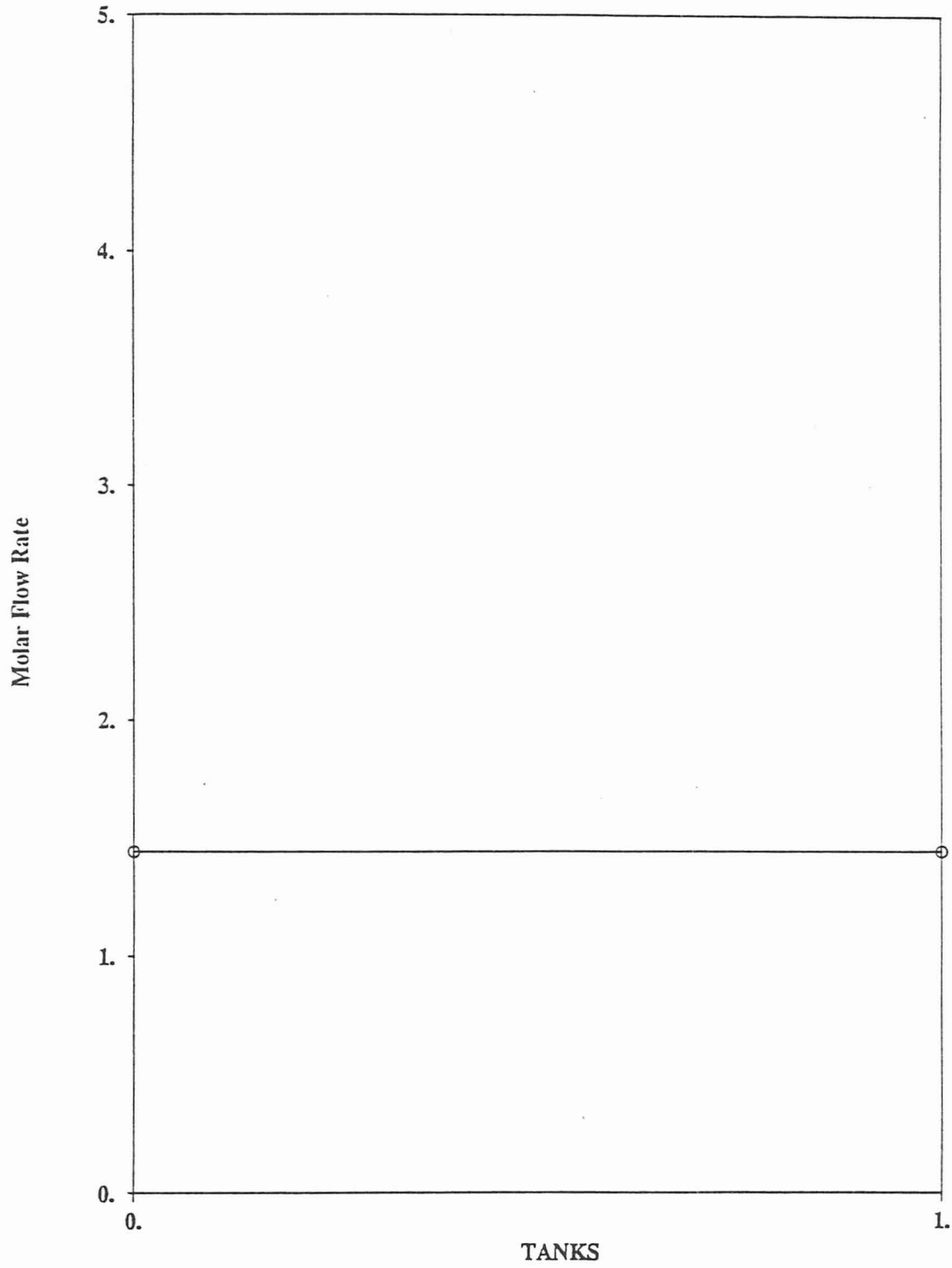


Figure 4.2: Case B

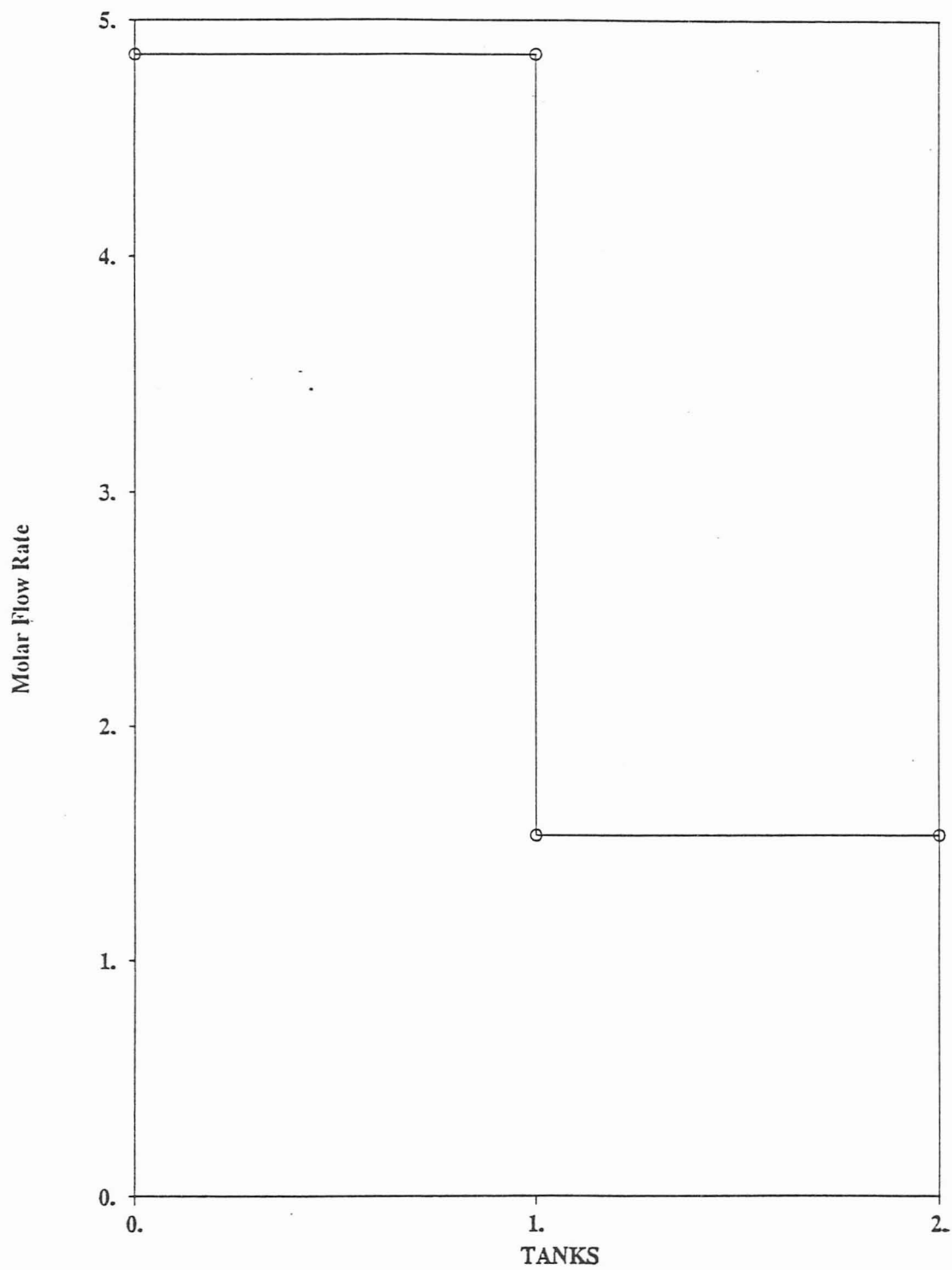


Figure 4.3: Case C

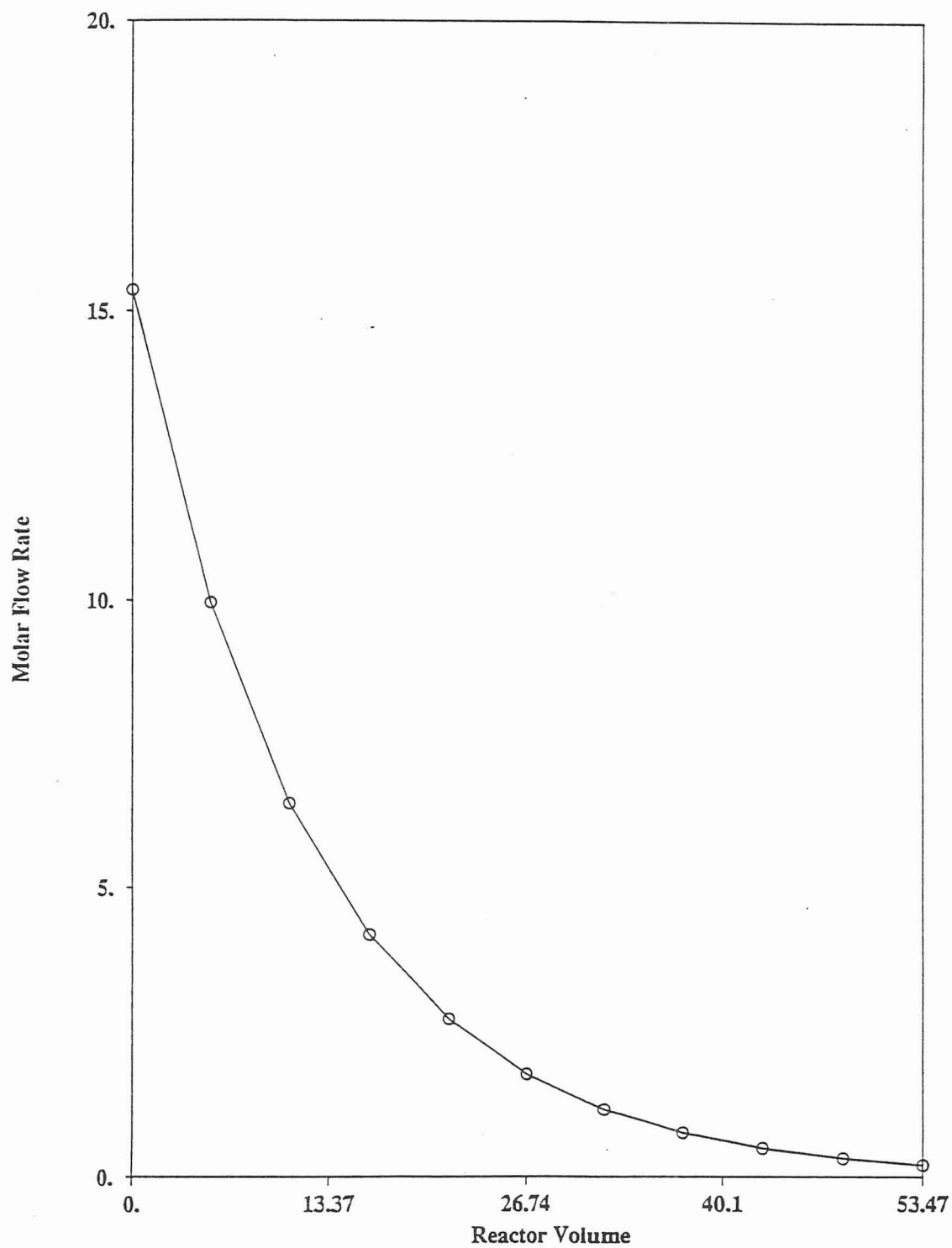


Figure 4.4: Case D

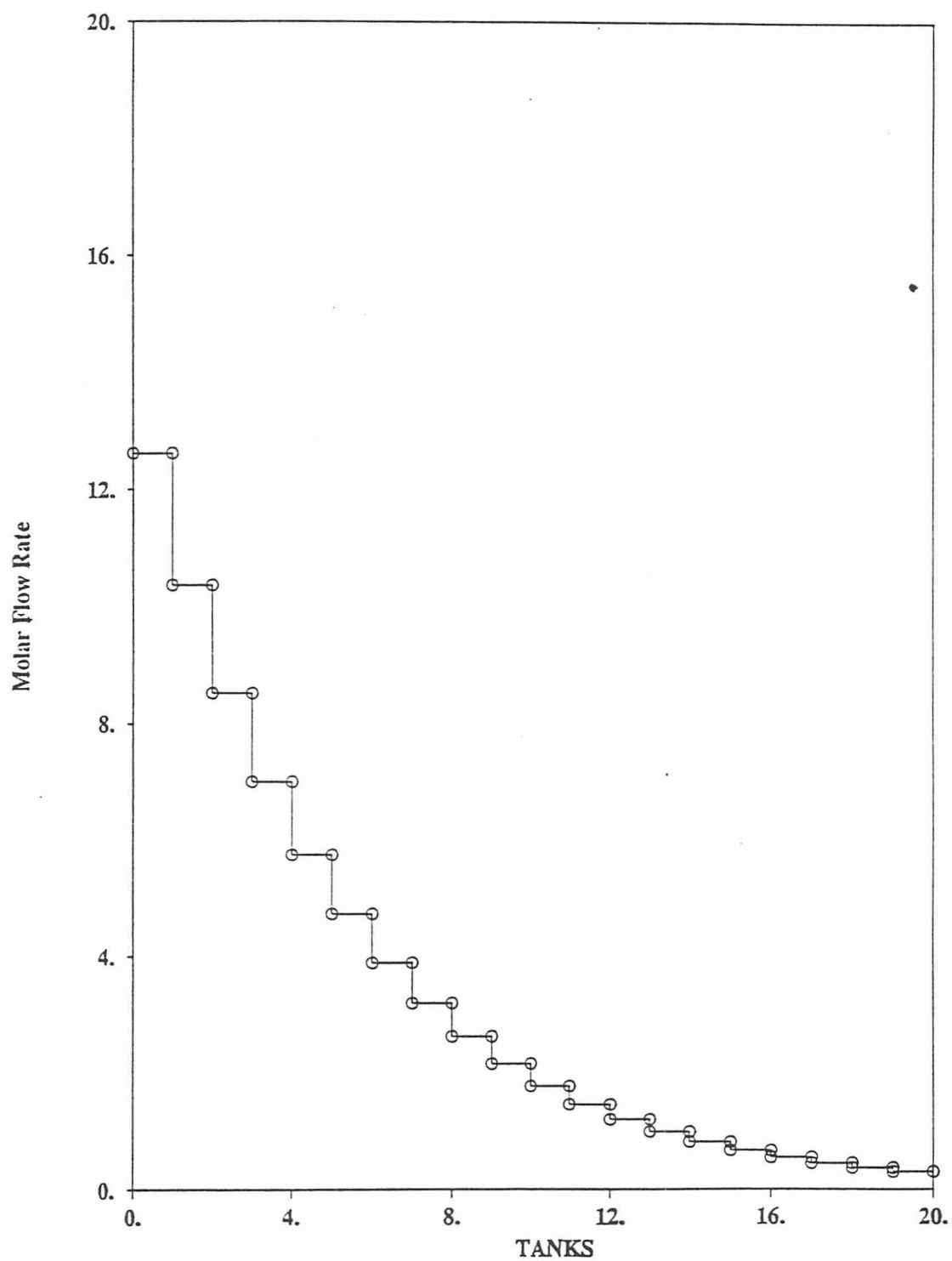


Figure 4.5: Case E

Chapter 5. Criteria

Criteria to estimate the importance of certain transport effects within chemical reactors are presented in this chapter. These criteria can be used to estimate when a particular phenomenon should be included in a reactor design. Specific criteria have been developed for: (1) heterogeneity, (2) density variations, and (3) radial dispersion. Heterogeneity includes heat and mass transfer resistance both internal and external to a catalyst. Density variations can arise from changes in pressure, temperature, and mole changes due to reaction. Density variations are most significant in gas-phase reactors. Radial dispersion is common in reactors with a large amount of heating or cooling at the wall. A fourth criterion is taken from the literature for axial dispersion. Axial dispersion is most common in reactors with a short length. These criteria will be used in chapters 6, 7, and 8 to compare with simulations run with CRDT. The criterion presented here are based on changes in concentration because a certain phenomenon is not considered important to the design if it does not change the amount of desired product by a significant measure.

5.1. Heterogeneity

The criterion to determine when heterogeneous effects become important was developed by solving equation describing a PFR presented in chapter 2, equation (2.15). This equation is solved assuming first order kinetics for two cases: case (1) without heterogeneous effects, case (2) with heterogeneous effects. Heterogeneous effects are accounted for by the use of the effectiveness factor, η . Recall the effectiveness factor is defined as the ratio of the rate of reaction with resistance to the rate of reaction with no resistance. The solution of equation (2.15) for case (1) and for case (2) is presented in equations (5.1) and (5.2). The concentrations in these equations are for the limiting reactant.

$$C_{a1} = C_{a0} \exp \left[\frac{\rho_B R_{a0} V}{F_{a0}} \right] \quad (5.1)$$

$$C_{a2} = C_{a0} \exp \left[\frac{\rho_B \eta R_{a0} V}{F_{a0}} \right] \quad (5.2)$$

The criterion is based on concentration of the limiting reactant. For the phenomenon to significantly affect the amount of the desired product, the concentration of the limiting reactant for case (2) should be within 5% of case (1). This criterion is stated mathematically in equation (5.3).

$$\left| \frac{C_{a2}}{C_{a1}} - 1 \right| < 0.05 \quad (5.3)$$

The combination of equations (5.1), (5.2), and (5.3) give the criterion for heterogeneity. This criterion predicts heterogeneous effects can be ignored if the effectiveness factor is within the range given in equation (5.4).

$$1 - \frac{0.05 F_{a0}}{\rho_B R_{a0} V} \leq \eta \leq 1 + \frac{0.05 F_{a0}}{\rho_B R_{a0} V} \quad (5.4)$$

5.2. Density Variations

The criterion for significance of density variations is developed in a similar manner. The equation for the PFR is again solved twice assuming first order kinetics. Case (1) assumes a constant velocity equal to the inlet velocity, $u_1 = u_0$. Case (2) assumes a constant velocity equal to an estimated outlet velocity. The outlet velocity is estimated by combining the continuity equation with the ideal gas law. The result is presented in equation (5.5).

$$u_2 = u_1 \frac{T_w P_0}{T_0 P_L (1 + \epsilon)} \quad (5.5)$$

The outlet temperature is assumed to approach the wall temperature. The outlet pressure is calculated assuming a linear pressure drop down the reactor length. The pressure gradient is found using equation (2.20). Changes in volume with mole change due to reaction is

also included. The parameters in equation (5.5) are given below.

T_w = Wall Temperature

$$P_L = P_0 - \left[\frac{dP}{dz} \right]_0 L$$

$$\epsilon_a = y_{a0} \delta$$

$$\delta = \sum_{j=1}^n \frac{v_j}{v_a}$$

The solution for this case (1) and case (2) is given in equations (5.6) and (5.7).

$$C_{a1} = C_{a0} \exp \left[\frac{\rho_B R_{a0} V}{u_1 A_c C_{a0}} \right] \quad (5.6)$$

$$C_{a2} = C_{a0} \exp \left[\frac{\rho_B \eta R_{a0} V}{u_2 A_c C_{a0}} \right] \quad (5.7)$$

The resulting criterion for density variations is found by combining equations (5.6) and (5.7) with equation (5.3). This criterion states that density variations do not significantly affect the amount of product if the ratio of the inlet velocity to the "outlet" velocity is within the range given in equation (5.8).

$$1 - \frac{0.05 F_{a0}}{\rho_B R_{a0} V} \leq \frac{u_1}{u_2} \leq 1 + \frac{0.05 F_{a0}}{\rho_B R_{a0} V} \quad (5.8)$$

5.3. Radial Dispersion

Developing a criterion to estimate the significance of radial dispersion is also done by solving the PFR equation for two cases. Temperature differences are the basis for this criterion. This is because the major factor contributing to radial dispersion is a radial temperature profile caused by heating or cooling at the wall. The radial temperature gradient forces a concentration gradient through the temperature dependence of the rate expression. This criterion is found by evaluating the rate constant at two temperatures. The solution for case (1) assumes no temperature gradient, using the inlet temperature, T_0 , for calculation of the rate constant. The solution for case (2) uses an average temperature, $\langle T \rangle$, for calculation of the rate constant. Equations (5.9) and (5.10) give the solution of

the PFR model for these two cases.

$$C_{a1} = C_{a0} \exp \left[\frac{\rho_B k_1(T_0) C_{a0} V}{F_{a0}} \right] \quad (5.9)$$

$$C_{a2} = C_{a0} \exp \left[\frac{\rho_B k_2(\langle T \rangle) C_{a0} V}{F_{a0}} \right] \quad (5.10)$$

The temperature for case (2) is the average temperature across the cross section of a model with radial dispersion. This two-dimensional reactor model is solved using a two-point orthogonal collocation solution (Finlayson 1980). This average temperature is defined mathematically in equation (5.11). T_1 and T_2 are the temperatures at collocation points 1 and 2, respectively.

$$\langle T \rangle = \frac{\int_0^{2\pi} \int_0^1 T(r) r \, dr \, d\theta}{\int_0^{2\pi} \int_0^1 r \, dr \, d\theta} = \frac{\sum w_j T_j}{\frac{1}{2}} = \frac{3}{4} T_1 + \frac{1}{4} T_2 \quad (5.11)$$

Orthogonal collocation applied to the boundary condition of the two-dimensional model results in equations (5.10) and (5.11).

$$-\sum A_{2,i} T_i = Bi_w (T_2 - T_w) \quad (5.12)$$

$$T_2 = \frac{3T_1 + Bi_w T_w}{3 + Bi_w} \quad (5.13)$$

Then, letting the temperature at the first collocation point equal the inlet temperature and combining equations (5.11) and (5.13) gives equation (5.14).

$$\langle T \rangle = \frac{3}{4} T_0 + \frac{3T_0 + Bi_w T_w}{12 + 4Bi_w} \quad (5.14)$$

The resulting criterion is found by combining equations (5.9) and (5.10) with equation (5.3). The criterion states that radial dispersion can be ignored if the ratio of two rate constants is within the range given by equation (5.15).

$$1 - \frac{0.05F_{a0}}{\rho_B R_{a0} V} \leq \frac{k_1(T_0)}{k_2(\langle T \rangle)} \leq 1 + \frac{0.05F_{a0}}{\rho_B R_{a0} V} \quad (5.15)$$

Note that the two rate constants will be equal if the wall temperature is equal to the inlet temperature, as is the case for the phthalic anhydride reactor in chapter 8. In that case, this criterion is inconclusive so a criterion from Mears (1971) can be employed instead.

This criterion predicts that at the hot spot, the average reaction rate at the cross section will differ from the local reaction rate at the wall by less than 5% if equation (5.16) is satisfied.

$$1 - \frac{0.4\lambda_{er}T_w}{(-\Delta H_{rxn})R_{a0}\gamma_w R^2} < \frac{4d_p}{Bi_w R} < 1 + \frac{0.4\lambda_{er}T_w}{(-\Delta H_{rxn})R_{a0}\gamma_w R^2} \quad (5.16)$$

Note that this criterion predicts fluctuations in reaction rates rather than in outlet concentrations.

5.4. Axial Dispersion

The criterion for axial dispersion is from Levenspiel and Bischoff (1963). For this criterion, the ratio of outlet concentration with axial dispersion to the outlet concentration without axial dispersion will vary by less than 5% if equation (5.17) is satisfied.

$$\frac{d_p L}{Pe_{m,a}} < 0.05 \left(\frac{\rho_B R_{a0}}{C_{a0} u_0} \right)^2 \quad (5.17)$$

Chapter 6. Sulfur Trioxide Reactor

This chapter shows the application of CRDT to the design of an industrial fixed-bed reactor. The various phenomena that can be studied individually with CRDT are compared to the *a priori* criteria predictions developed in the previous chapter. This comparison illustrates the effectiveness of the *a priori* predictions. The usefulness of CRDT as a design tool is demonstrated by investigating the importance of each phenomenon.

The oxidation of sulfur dioxide to sulfur trioxide is studied using the following models: the PFR, the PFR with axial dispersion, and the tubular reactor with radial dispersion. To compare the two-dimensional model to the one-dimensional models, the wall heat transfer coefficient, h_w , needs to be correlated to the overall heat transfer coefficient, U . Young and Finlayson (1973) provide the relation given in equation (6.1).

$$\frac{1}{U} = \frac{1}{h_w} + \frac{R_t}{3\lambda_{er}} \quad (6.1)$$

The effects of heterogeneity and density variations are investigated along with this reactor model comparison. The total concentration (density) can be assumed constant, or it can vary due to temperature, pressure, and/or mole changes due to reaction. When the density varies, the velocity also varies to satisfy the continuity equation.

$$\rho u A_c = \text{constant} \quad (6.2)$$

Heterogeneous effects require the reaction rate to be evaluated at the concentrations and temperature at the surface of the catalyst. For mass and heat transfer resistance external to the catalyst the reaction rates along with the surface concentrations and temperature are determined by solving the set of algebraic equations given in equations (2.27) and (2.28). The reaction rate routine uses effectiveness factors to account for mass and heat transfer resistance internal to the catalyst. For the sulfur trioxide reaction system studied, the catalyst is non-porous, therefore only external resistance needs to be investigated.

Below, the reaction system and rate expression for the oxidation of sulfur dioxide

to sulfur trioxide with a platinum coated catalyst is presented (Young and Finlayson 1973).



$$r_1 = \frac{X\sqrt{1 - 0.166(1 - X)} - 2.2(1 - X)/K_{\text{eq}}}{(k_1 + k_2(1 - X))^2} [=] \frac{\text{kmol}}{\text{kgcat.hr.}} \quad (6.3)$$

The rate parameters are given in equation (6.4)

$$\begin{aligned} k_1 &= \exp\left(-14.96 + \frac{11070}{T(\text{K})}\right) & k_2 &= \exp\left(-1.331 + \frac{2331}{T(\text{K})}\right) \\ K_{\text{eq}} &= \exp\left(-11.02 + \frac{11570}{T(\text{K})}\right) & \Delta H_{\text{rxn},1} &= -97,500 \text{ KJ/Kmol} \end{aligned} \quad (6.4)$$

Ten simulations outlined in table 6.1 were run for the sulfur trioxide reactor using CRDT. These simulations allow for comparison of reactor type and comparison of the various phenomena considered. Note, the simulations listed do not include the effects of pressure drop or density variations for the two-dimensional reactor. For this reaction system, simulations for the two-dimensional reactor with variable density produce non-physical results. The concentrations near the wall become negative at a dimensionless length of 0.8. This can be attributed to the fact that the model for the two-dimensional reactor allows concentrations and temperatures to be a function of radial location. Pressure is treated as constant across the radius. The total concentration varies radially so the ideal gas law is always satisfied. A more appropriate model would include the possibility of radial variations in pressure. This can be accomplished by including a momentum balance.

The values of the model parameters are given in table 6.2. These parameters are used as input for CRDT and for the calculation of the criteria developed in the previous chapter. The FORTRAN rate expression is given in appendix B.

The results of the criterion estimates for the sulfur trioxide reactor are presented in table 6.3. If the value of the criterion is between the lower and upper limits, then that phenomenon will not affect the outlet concentration of limiting reactant by more than 5%. Notice the parameters in the bounds of the criteria are equivalent in equations (5.4), (5.8),

and (5.15). The ratio of the parameters is a Damköhler number based on the limiting reactant. This ratio can be calculated using the mole fraction and Damköhler number given in table 6.2 as illustrated in equation (6.5).

$$\frac{F_{a0}}{\rho_B R_{a0} V} = \frac{y_{a0}}{Da_I} \quad (6.5)$$

Figure 6.1 is a plot of the conversion of SO_2 versus the reactor length.

Experimental data from Schuler, *et al.*, (1954) are included in figure 6.1. Figure 6.2 shows the temperature as a function of reactor length for the three reactor types. The conversion and temperature are averaged across the reactor radius for the two-dimensional simulations. Experimental data for the temperature at the centerline agrees with the temperature at the centerline for the two-dimensional simulation but is not shown. Conversion in simulation 3 is 26% higher than in simulation 10, showing the effect of a two-dimensional reactor. One would expect that the two-dimensional model will give different results than a one-dimensional model based on the high value of the Biot number for this reactor. The significance of radial dispersion can be demonstrated further by comparing the magnitudes of the three terms in equation (2.6). Figure 6.3 presents a three-dimensional representation of the convection, dispersion, and rate terms. The z-axis represents the dimensionless magnitude of each term of the SO_3 mass balance equation. Note the dispersion term is significant throughout the length of the reactor. Also, there are significant radial profiles in the convective and rate terms.

Figures 6.1 and 6.2 also suggest that axial dispersion may be important in this reactor. The conversion in simulation 3 is 7% greater than the conversion from simulation 7. The significance of axial dispersion in this reactor can be attributed to the short length of this reactor. Notice that the curvature of the axial dispersion model closely follows the curvature of the experimental data. This suggests that a model including both axial dispersion and radial dispersion will represent the experimental data better than either of the

individual models. This was confirmed by Young and Finlayson (1973).

Density and heterogeneous effects are studied using the PFR model. Figure 6.4 is a plot of conversion versus reactor length. Conversion of SO_2 is reduced by 8% when heterogeneous effects are included in the model. This suggests, along with the agreement of the experimental data with simulation 10 in figure 6.1, that heterogeneous effects need to be accounted for in the model for this reactor.

Including density variations in the model reduce conversion of SO_2 by 5%. This result can be attributed to the large temperature difference between the inlet and wall temperatures. Mole changes due to reaction magnify the effect. Pressure drop is negligible in this reactor due to the short length and low Reynolds' number. Including both density variation and heterogeneous effects in the model results in a 12% decrease in conversion of SO_2 . Thus, the results of the simulations suggest that the appropriate model for this reactor is a tubular flow reactor including both axial dispersion and radial dispersion, heterogeneous effects, and density variations.

Table 6.4 compares the results from the simulations to the criteria's predictions and the models from the previous study. Recall that the concentration out of the reactor had to vary by more than 5% for the phenomena to be important enough to include in the model. The model used by Young and Finlayson included all the phenomena except their model assumed constant total concentration. The criteria predicted all of the phenomena to be important. The results of the simulations performed with CRDT agree with the criteria's predictions.

From these results, it can be concluded that CRDT is effective in analyzing the many phenomena that can have an impact on the results of a chosen reactor model. This chapter has also demonstrated that the criterion developed in chapter 5 is useful in estimating the importance of the phenomenon studied. With the criterion estimates and CRDT, the appropriate model can be chosen for the sulfur trioxide reactor.

Table 6.1.--Simulations

Number	Description
1	PFR - Total concentration constant - Homogeneous
2	PFR - Total concentration varies - Homogeneous
3	PFR - Total concentration constant - Heterogeneous
4	PFR - Total concentration varies - Heterogeneous
5	PFR with axial dispersion - Total concentration constant - Homogeneous
6	PFR with axial dispersion - Total concentration varies - Homogeneous
7	PFR with axial dispersion - Total concentration constant - Heterogeneous
8	PFR with axial dispersion - Total concentration varies - Heterogeneous
9	2-D reactor - Total concentration constant - Homogeneous
10	2-D reactor - Total concentration constant - Heterogeneous

Table 6.2.--Parameters for Sulfur Trioxide Reactor

Parameter	Value	Parameter	Value
L (m)	0.15	λ_{er} (KJ/msK)	0.00049
R (m)	0.026	λ_{ez} (KJ/msK)	0.0016
d_p (m)	0.0032	$Pe_{h,r}$	3.23
ϵ	0.43	$Pe_{h,L}$	45.9
y_{a0}	0.065	Bi	10
T_0 (K)	673	U (KJ/m ² sK)	0.042
T_w (K)	470	St	1.02
P_0 (atm)	1.0	Da_I	0.15
G (Kg/m ² s)	0.475	Da_{III}	0.70
Re	46	k_{ma} (/s)	186
$Pe_{m,r}$	9.6	h_{pa} (KJ/m ³ sK)	251
$Pe_{m,L}$	93.8	$dP/dz _0 * L/P_0$	-0.005

Table 6.3.--Criterion Results for the Sulfur Trioxide Reactor

Phenomenon	Criterion Value	Lower Limit	Upper Limit	Important?
Radial Dispersion	0.13	0.98	1.02	Yes
Axial Dispersion	0.0024	0	0.0021	Yes
Heterogeneity	1.06	0.98	1.02	Yes
Density Variations	1.38	0.98	1.02	Yes

Table 6.4.--Importance of Phenomena in Sulfur Trioxide Reactor

Phenomenon	Literature	Criterion	CRDT
Radial Dispersion	Yes	Yes	Yes
Axial Dispersion	Yes	Yes	Yes
Heterogeneity	Yes	Yes	Yes
Density Variations	No	Yes	Maybe

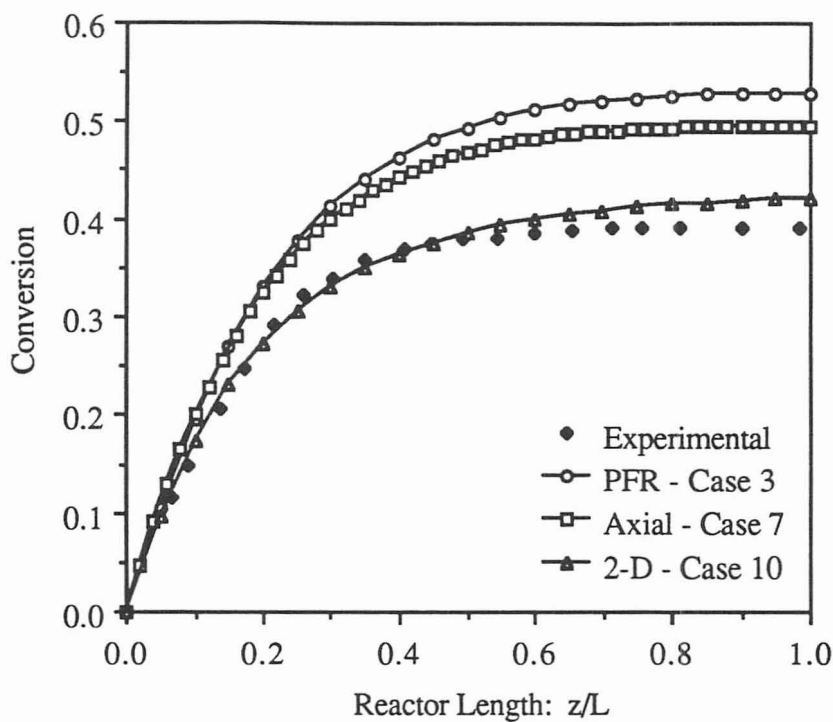


Figure 6.1: Conversion for the Sulfur Trioxide Reactor Comparison. Experimental Data from Schuler, *et al.* (1954)

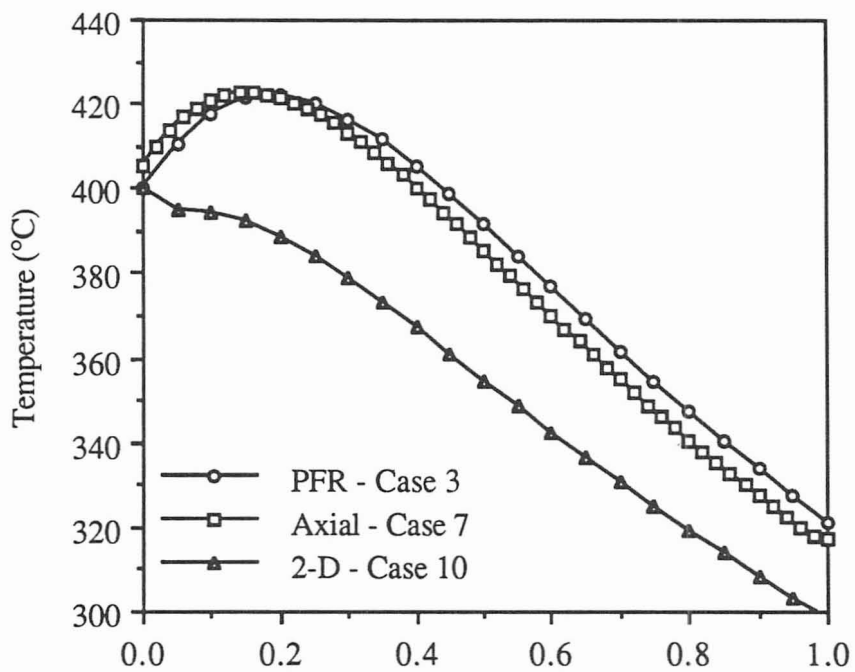


Figure 6.2: Temperature Profiles for the Sulfur Trioxide Reactor Comparison

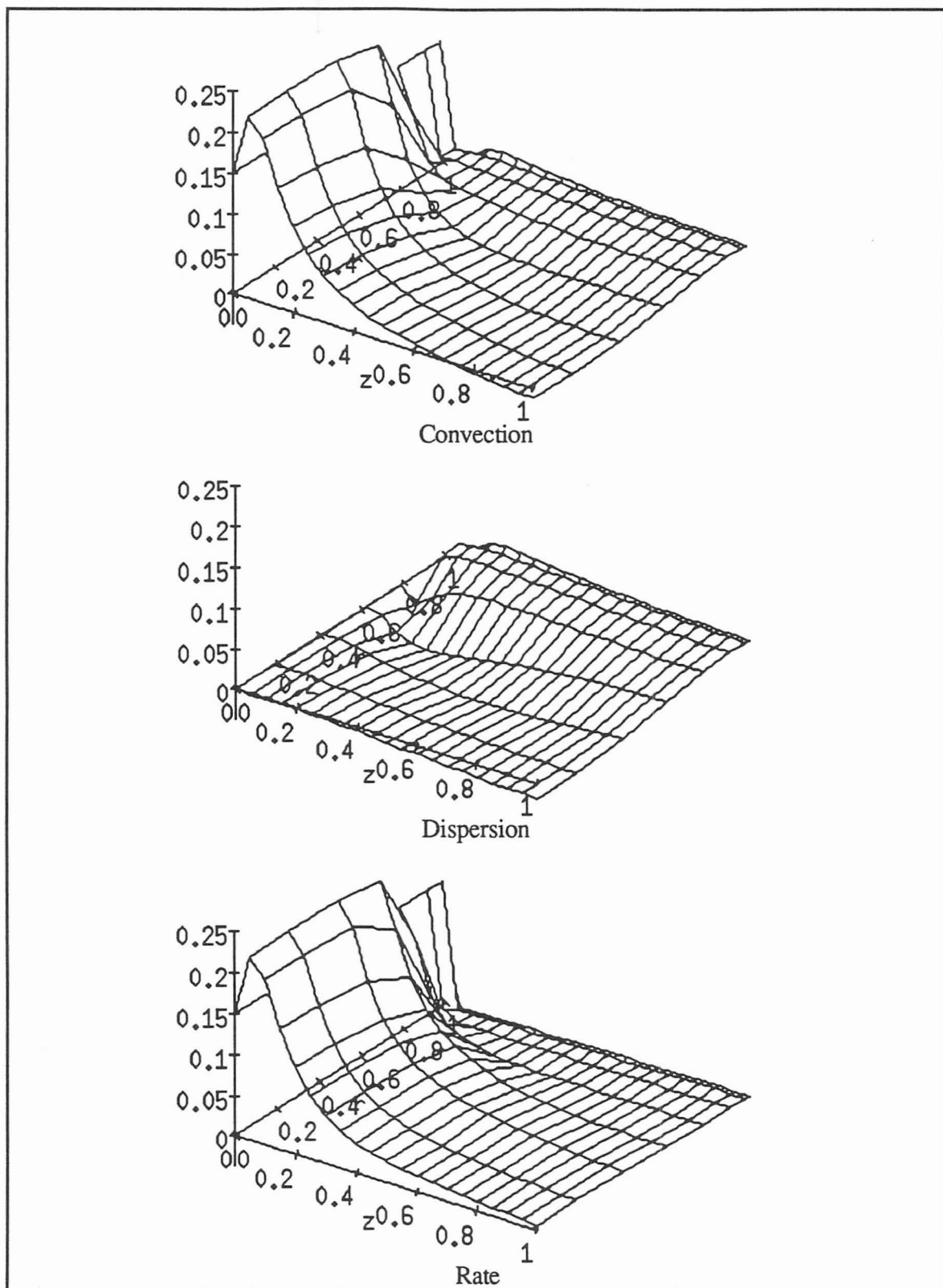


Figure 6.3: Convection, Dispersion, and Rate Terms for the Sulfur Trioxide Mass Balance

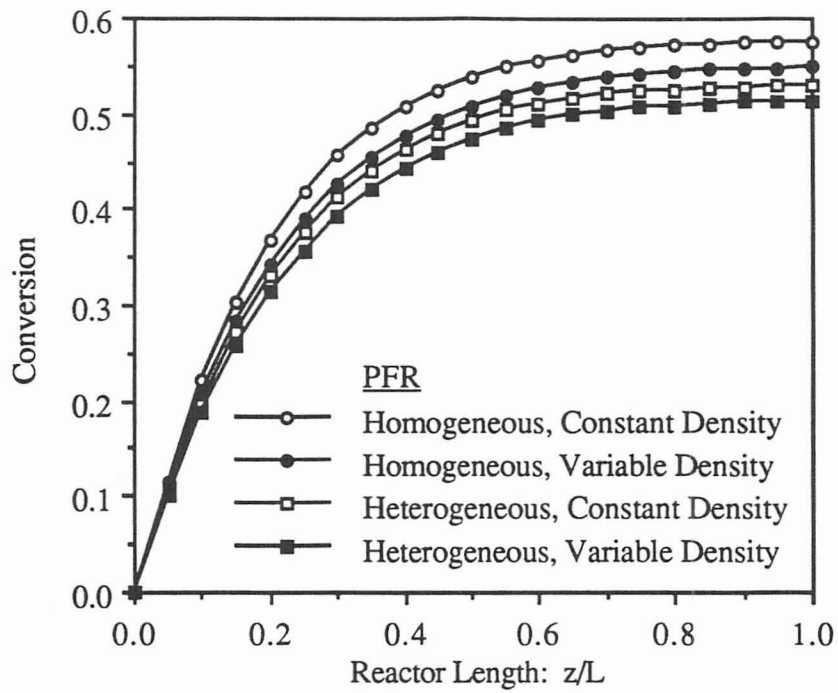


Figure 6.4: Comparison of Conversion for Various Effects in the Sulfur Trioxide Reactor. Simulations 1, 2, 3, and 4.

Chapter 7. Phthalic Anhydride Reactor

Another application of CRDT to the design of an industrial fixed-bed reactor is presented in this chapter. The various phenomena studied individually with CRDT are again compared to the *a priori* criteria's predictions developed in chapter 5. The results of CRDT are compared with the predictions of the criteria. This comparison illustrates further the effectiveness and limitations of the *a priori* predictions and the usefulness of CRDT as a design tool.

In this chapter, the oxidation of o-xylene to phthalic anhydride is studied using the PFR, PFR with axial dispersion, and the two-dimensional reactor models. The comparison of the two-dimensional model to the one-dimensional models requires correlating the wall heat transfer coefficient to the overall heat transfer coefficient. For this reaction system, this is accomplished by using the correlation in equation (7.1) from Froment and Bischoff (1990).

$$\frac{1}{U} = \frac{1}{h_w} + \frac{R_t}{4\lambda_{er}} \quad (7.1)$$

Heterogeneous effects and density variations are also investigated. Mass and heat transfer resistance external to the catalyst were calculated using correlations from literature shown in equations (7.2) to (7.4). (Froment and Bischoff 1990).

$$j_D = 1.66\text{Re}^{-0.51} \quad (7.2)$$

$$j_D = \frac{k_g M_m c_{fi}}{G} \text{Sc}^{2/3} \quad (7.3)$$

$$j_D = \frac{h_f}{c_p G} \text{Pr}^{2/3} \quad (7.4)$$

The reaction system and rate expressions for the oxidation of o-xylene to phthalic anhydride are given below (Froment and Bischoff 1990).



$$r_1 = k_1 p_{\text{oxy}} p_{\text{O}_2} \quad [=] \quad \frac{\text{kmol}}{\text{kgcat.hr.}} \quad \Delta H_{\text{rxn},1} = 1,285,000 \text{ KJ/kmol} \quad (7.5)$$

$$r_2 = k_2 p_{\text{pa}} p_{\text{O}_2} \quad \Delta H_{\text{rxn},2} = 3,279,000 \text{ KJ/kmol}$$

$$r_3 = k_3 p_{\text{oxy}} p_{\text{O}_2} \quad \Delta H_{\text{rxn},3} = 4,564,000 \text{ KJ/kmol}$$

The parameters for the rate expression are given in equation (7.6).

$$k_1 = \exp\left(19.837 - \frac{13588}{T(\text{K})}\right) \quad k_2 = \exp\left(20.86 - \frac{15803}{T(\text{K})}\right) \quad (7.6)$$

$$k_3 = \exp\left(18.97 - \frac{14394}{T(\text{K})}\right)$$

The ten simulations outlined in table 6.1 were also run for this reaction system. Again, results of the simulations are not included for pressure drop or density variations in the two-dimensional reactor. This reaction system also produces non-physical results for the two-dimensional reactor with variable density. Table 7.1 provides the parameters required by CRDT and required for the calculation of the criteria. The predictions from the criteria are given in table 7.2. The phenomenon should not affect the outlet concentration of limiting reactant by more than 5% if the value of the criterion falls between the lower and upper limits. Note that the estimate for radial dispersion is calculated using the criterion from Mears (1971) since the wall and inlet temperatures are equal for this design. The FORTRAN rate expression for this system can be found in appendix B.

Figure 7.1 is a plot of conversion against reactor length for the three reactor types. The PFR and axial dispersion models give the same conversion. The conversion is 3% greater in the two-dimensional model than in the one-dimensional models. Selectivity is a better measure of the performance of the reactor since side reactions occur in this reaction system. Equation (7.7) defines the selectivity as the ratio of moles of desired product to the

moles of reactant converted.

$$S = \frac{F_{PA}}{F_{PA} + F_{CO_2}} \quad (7.7)$$

Figure 7.2 and 7.3 show the selectivity and temperature profiles versus the reactor length for the three reactor types. Data from simulations performed by the previous investigators are also presented in Figure 7.3. Again, there is little difference between the PFR and axial dispersion models. The selectivity in the two-dimensional model is less than 1% lower than the one-dimensional simulations. The average temperature in the two-dimensional simulation is greater at the hot-spot than the temperatures in simulations 3 and 7. Thus, it can be concluded that axial dispersion and radial dispersion have no significant effect on the amount of phthalic anhydride produced in the reactor models. However, the two-dimensional model does show a significant radial temperature profile as can be seen in figure 7.4. Radial dispersion does affect the temperature profile but the influence on conversion and selectivity is negligible.

Heterogeneity and density variations are studied using the PFR model. The selectivity is plotted against reactor length in figure 7.5. Heterogeneity and density variations influence the selectivity by less than 1%. Notice that the two effects cancel each other; the simulation where both effects are included gives nearly the same profile as the simulation where neither was included. Thus, the results of CRDT's simulations suggest the PFR without heterogeneous effects and with constant total concentration is a sufficient model for prediction of the amount of phthalic anhydride produced by this reactor. If an accurate measure of the temperature profile in the reactor is desired, then the two-dimensional model should be used. Froment and Bischoff (1990) also compare the two-dimensional model with a one-dimensional model. They also conclude that a one-dimensional model can give accurate results.

The criteria's predictions are compared with the results of the simulations and the

literature model in table 7.3. Recall that the criterion for radial dispersion for this reactor is based on the energy balance at the hot-spot. It predicts radial dispersion will be important at the hot spot. This is true and is demonstrated in figure 7.4. What this criterion fails to predict is if the importance of radial dispersion at the hot spot has any affect on the conversion or selectivity. Figure 7.1 and 7.2 show that it does not.

Table 7.1.--Parameters for Phthalic Anhydride Reactor

Parameter	Value	Parameter	Value
L (m)	3.0	λ_{er} (KJ/msK)	0.00078
R (m)	0.0127	λ_{ez} (KJ/msK)	0.0034
d_p (m)	0.003	$Pe_{h,r}$	5.25
ϵ	0.5	$Pe_{h,L}$	1210
y_{a0}	0.00924	Bi	2.54
T_0 (K)	628	U (KJ/m ² sK)	0.0845
T_w (K)	628	St	29.0
P_0 (atm)	1.0	Da_I	0.0078
G (Kg/m ² s)	1.3	Da_{III}	0.516
Re	121	k_{ma} (/s)	74
$Pe_{m,r}$	10	$h_{p,a}$ (KJ/m ³ sK)	290
$Pe_{m,L}$	1000	$dP/dz _0 * L/P_0$	-0.054

Table 7.2.--Criterion Results for the Phthalic Anhydride Reactor

Phenomenon	Criterion Value	Lower Limit	Upper Limit	Important?
Radial Dispersion	0.37	0.62	1.4	Yes
Axial Dispersion	0.009	0	0.63	No
Heterogeneity	0.99	0.94	1.06	No
Density Variations	0.95	0.94	1.06	No

Table 7.3.--Importance of Phenomena in Phthalic Anhydride Reactor

Phenomenon	Literature	Criterion	CRDT
Radial Dispersion	Yes	Yes	Maybe
Axial Dispersion	No	No	No
Heterogeneity	No	No	No
Density Variations	No	No	No

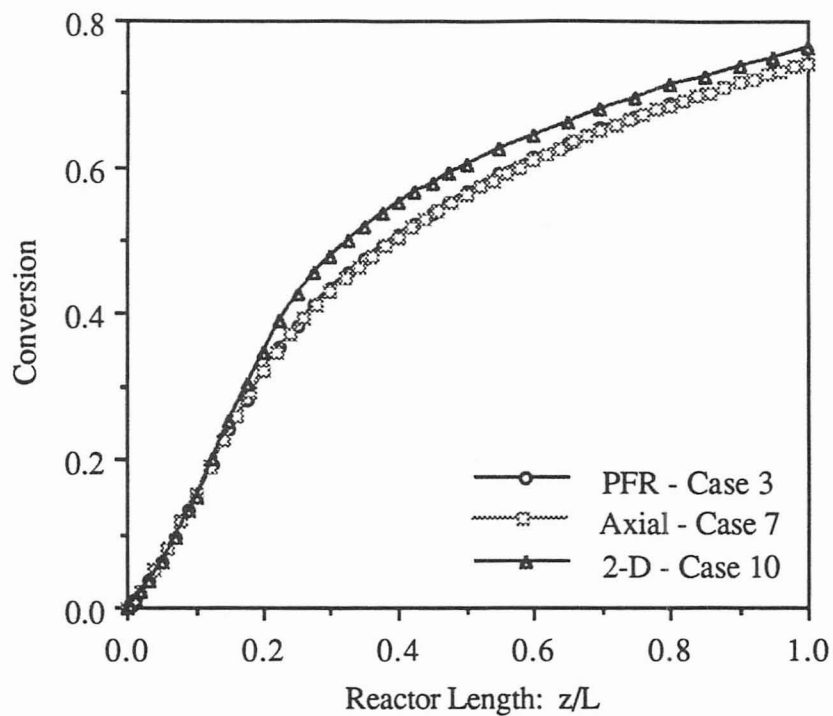


Figure 7.1: Conversion for the Phthalic Anhydride Reactor Comparison

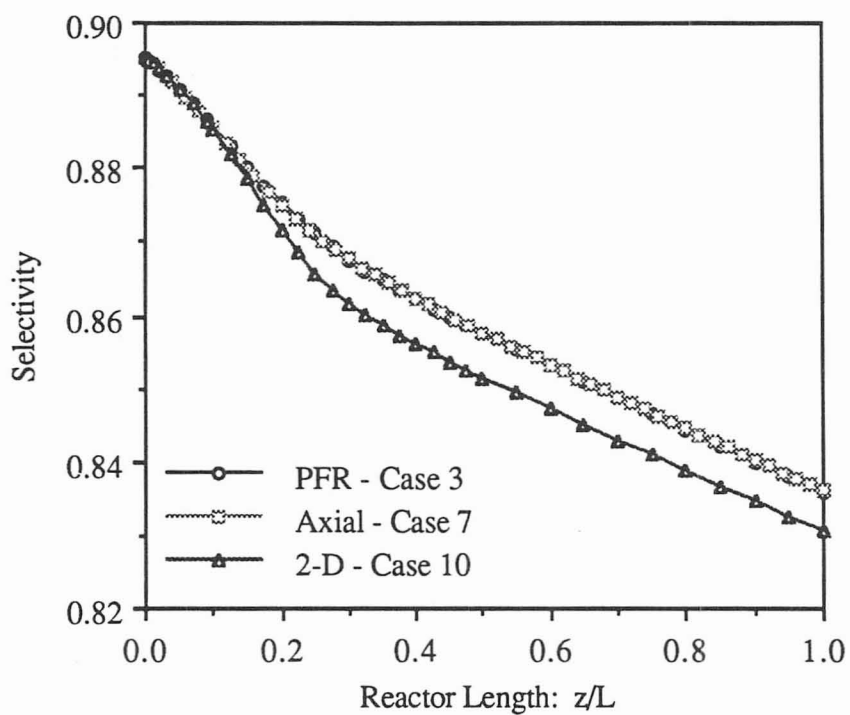


Figure 7.2: Selectivity for the Phthalic Anhydride Reactor Comparison

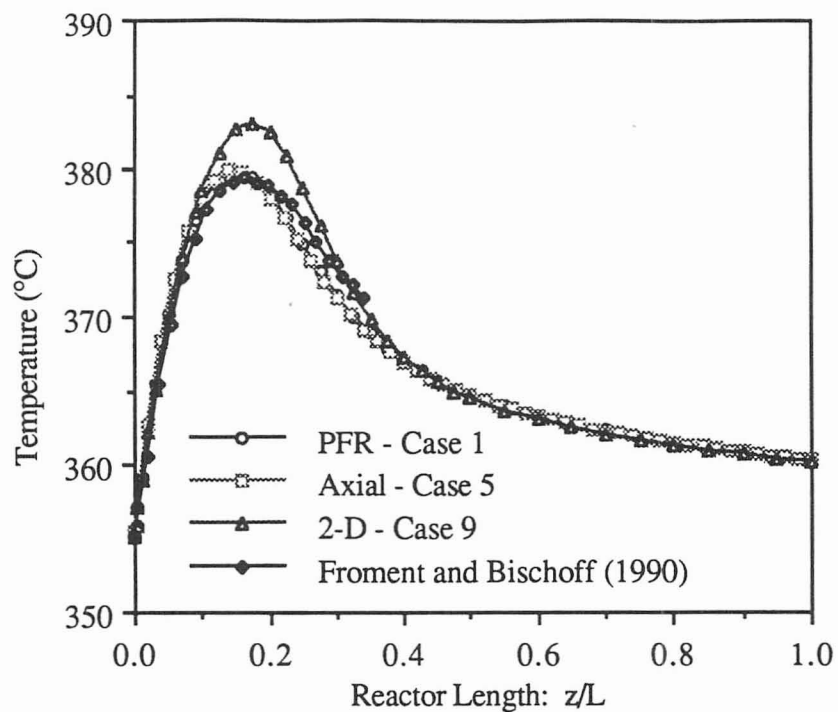


Figure 7.3: Temperature Profiles for the Phthalic Anhydride Reactor Comparison

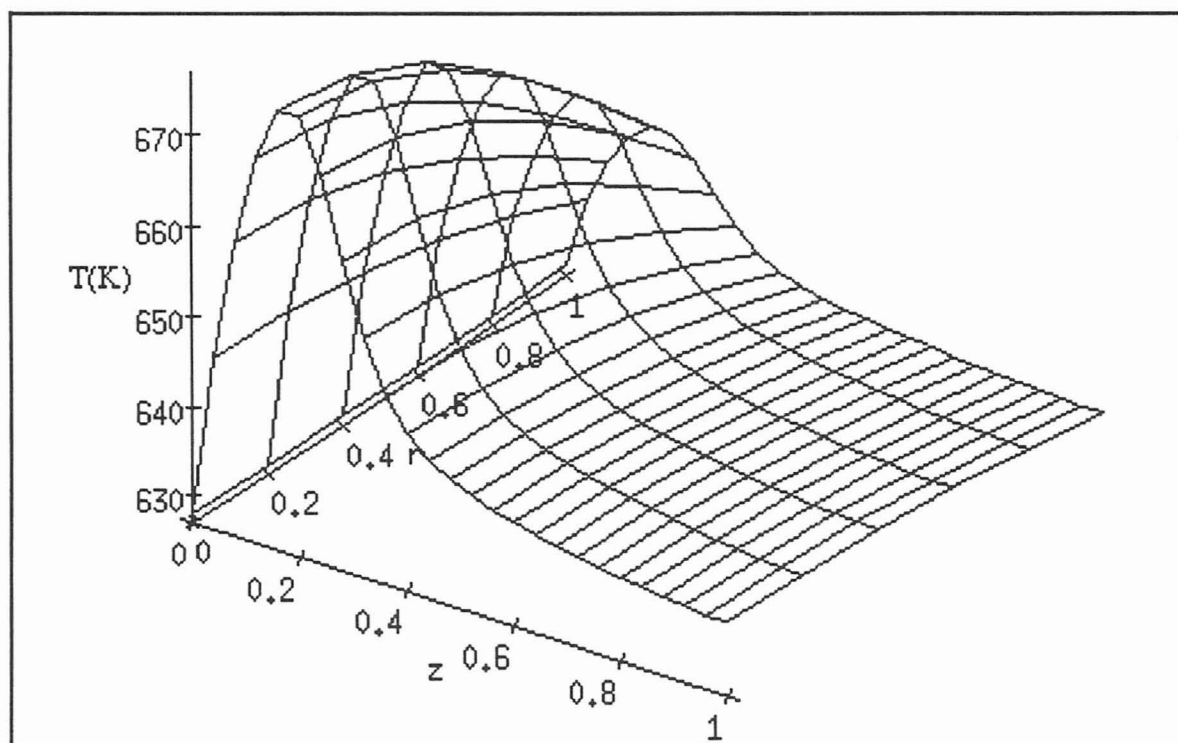


Figure 7.4: Temperature Profile in the Phthalic Anhydride 2-D Reactor

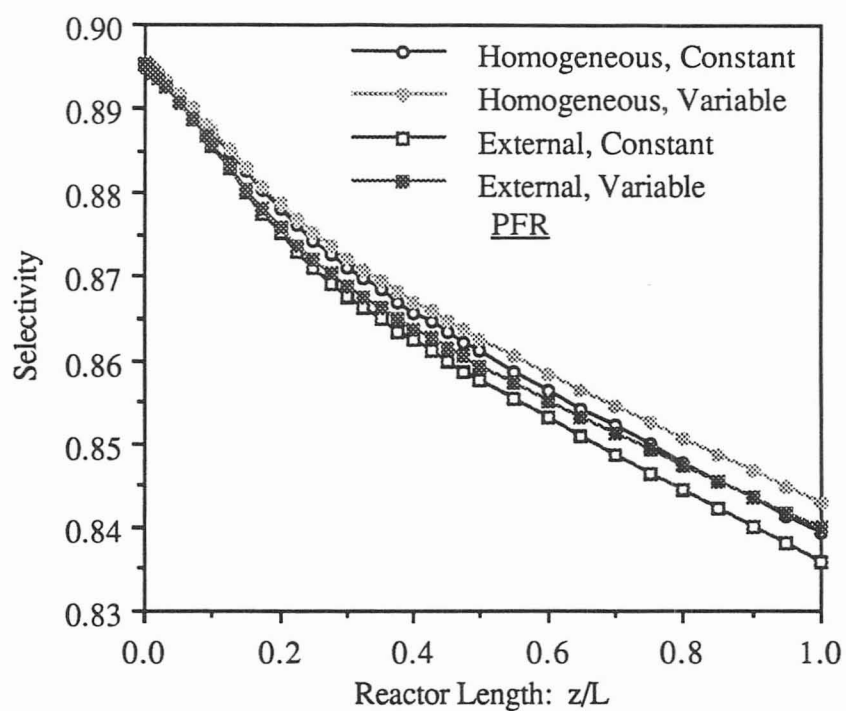


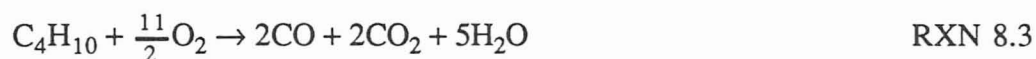
Figure 7.5: Selectivity Comparison for Various Effects in the Phthalic Anhydride Reactor. Simulations 1, 2, 3, and 4.

Chapter 8. Maleic Anhydride Reactor

A third application of CRDT to the design of an industrial fixed-bed reactor is presented in this chapter. The various phenomena studied individually with CRDT are again compared to the *a priori* criteria developed in chapter 5. The results of CRDT are compared with the predictions of the criteria. This final comparison further illustrates the usefulness of CRDT as a design tool and the effectiveness and limitations of the *a priori* predictions.

In this chapter, the oxidation of n-butane to maleic anhydride is studied using the PFR, PFR with axial dispersion, and the two-dimensional reactor models. The comparison of the two-dimensional model to the one-dimensional models requires correlating the wall heat transfer coefficient to the overall heat transfer coefficient. For this reaction system, this is accomplished by using the correlation given in chapter 6, equation (6.1). Heterogeneous effects and density variations are also investigated. Effectiveness factors for resistance internal to the catalyst were provided by Sharma, *et al.* (1991). CRDT incorporates internal resistance in the FORTRAN rate expression (see appendix B). Resistance external to the catalyst was determined unimportant by CRDT using coefficients calculated with equations (7.2) to (7.4).

Below, the reaction system and rate expression for the oxidation of n-butane to maleic anhydride with a vanadium-phosphor oxide catalyst are presented (Sharma, *et al.* 1991).



$$r_1 = \frac{k_1 P_{\text{but}}^{0.54}}{1 + 310 P_{\text{ma}}} [=] \frac{\text{kmol}}{\text{kgcat.s}} \quad \Delta H_{\text{rxn},1} = 1,239,000 \text{ KJ/kmol} \quad (8.1)$$

$$r_2 = \frac{k_2 P_{\text{ma}}}{(1 + 310 P_{\text{ma}})} \quad \Delta H_{\text{rxn},2} = 281,000 \text{ KJ/kmol}$$

$$r_3 = k_3 P_{\text{but}}^{0.54} \quad \Delta H_{\text{rxn},3} = 2,087,000 \text{ KJ/kmol}$$

The parameters for the rate expression are given in equation (8.2) through (8.4).

$$k_1 = 0.96 \times 10^{-6} \exp \left[\frac{93100}{673R} \left(1 - \frac{673}{T(\text{K})} \right) \right] \quad (8.2)$$

$$k_2 = 0.29 \times 10^{-5} \exp \left[\frac{155000}{673R} \left(1 - \frac{673}{T(\text{K})} \right) \right] \quad (8.3)$$

$$k_3 = 0.15 \times 10^{-6} \exp \left[\frac{93100}{673R} \left(1 - \frac{673}{T(\text{K})} \right) \right] \quad (8.4)$$

The same ten simulations outlined in chapter 6, table 6.1, were run for this reaction system but the heterogeneous effects are internal resistance rather than external resistance. Results of the simulations are not included for pressure drop or density variations in the two-dimensional reactor. This reaction system also produces non-physical results for the two-dimensional reactor with variable density. Again, these simulations are used to compare reactor type and the effects of density variations and heterogeneity. The results of these simulations are then compared to the predictions of the criteria and experimental data. Using all this information, the simplest model that will accurately predict outlet concentration can be chosen.

The parameter values required by CRDT and for the calculation of the criteria are given in table 8.1. The results of the criteria's predictions are given in table 8.2. If the value of the criterion falls between the lower and upper limits, then that phenomenon will not affect the outlet concentration of the limiting reactant by more than 5%. It should be noted that the values for this reactor were not calculated at the inlet temperature. No reaction occurs at the inlet temperature. The reaction initiates at about 565 K, so the criterion values were calculated at the initiation temperature. The initiation temperature was

also chosen as the standard for non-dimensionalization, thus the parameters in table 8.1 are the correct parameters to use for calculation of the criterion values.

Figure 8.1 show the results of the reactor comparison. Selectivity for this reaction system is the amount of n-butane converted to maleic anhydride defined below in equation (8.5).

$$S = \frac{F_{ma}}{F_{ma} + \frac{1}{4}(F_{co} + F_{co_2})} \quad (8.5)$$

Figure 8.2 shows the temperature profiles in the reactor for the three reactor types along with experimental data from Sharma, *et al.* (1991). From these two figures, it can be concluded that axial dispersion and radial dispersion have no significant influence on the selectivity or temperature. This is true for conversion of reactant also and is shown in figure 8.3.

Figures 8.4 and 8.5 show the significance of heterogeneity and density variation on the conversion and selectivity. Including heterogeneous effects reduced conversion by 6% and the selectivity by 5% for the PFR model. Accounting for the variations in density resulted in a 1% reduction in conversion but a 2.5% increase in selectivity. This can be attributed to the pressure drop in the reactor. The ratio of the pressure out of the reactor to the pressure into the reactor is 0.65. With the reduced pressure, the conversion will be preferential to the reaction producing the fewer number of moles. The desired reaction, RXN 8.1, produces the fewer number of moles in this system resulting in the increase in selectivity with the reduction in pressure.

Table 8.3 compares the results of the simulations done with CRDT to the criteria's predictions and the literature model. The criteria for radial dispersion and for heterogeneity are borderline values, shown in table 8.2. Including heterogeneous effects in the simulations resulted in concentration differences of about 5%. Since this value is the limit on the criterion, it is natural to obtain borderline predictions. The borderline prediction of

the radial dispersion effects is not as easily explained. The previous investigators also suggest that radial dispersion may be important in this reactor, but do not include it in their model. Figure 8.5 is a three-dimensional representation of the convection, dispersion, and rate terms for this reactor. The dispersion term is significant early in the reactor at the point of reaction initiation. The dispersion term goes to zero after the reaction is initiated and stays at zero throughout the rest of the reactor. This explains why there is little influence on the conversion or selectivity. The criterion predicts dispersion to be important because the criterion was calculated at the initiation temperature for this reactor.

The results of the simulations for the maleic anhydride reactor suggest that a one-dimensional plug flow model including heterogeneous effects is a sufficient model for this reaction system. However, the significant pressure drop needs to be included in the model. Thus, density variations may as well be included in the model since the model is already solving for both pressure and temperature.

Table 8.1.--Parameters for Simulations

Parameter	Value	Parameter	Value
L (m)	5.0	λ_{er} (KJ/msK)	0.0011
R (m)	0.0125	λ_{ez} (KJ/msK)	0.0029
d_p (m)	0.003	$Pe_{h,r}$	3.79
ϵ	0.44	$Pe_{h,L}$	2360
y_{a0}	0.0186	Bi	1.9
T_0 (K)	450	U (KJ/m ² sK)	0.104
T_w (K)	663	St	61.0
P_0 (atm)	1.65	Da_I	0.00306
G (Kg/m ² s)	1.25	Da_{III}	0.205
Re	121	k_{ma} (/s)	--
$Pe_{m,r}$	8	h_{pa} (KJ/m ³ sK)	--
$Pe_{m,L}$	1667	$dP/dz _0 * L/P_0$	-0.19

Table 8.2.--Criterion Results for the Maleic Anhydride Reactor

Phenomenon	Criterion Value	Lower Limit	Upper Limit	Important?
Radial Dispersion	1.4	0.67	1.33	Maybe
Axial Dispersion	0.015	0	83.8	No
Heterogeneity	0.62	0.67	1.33	Maybe
Density Variations	0.69	0.67	1.33	No

Table 8.3.--Importance of Phenomena in Maleic Anhydride Reactor

Phenomenon	Literature	Criterion	CRDT
Radial Dispersion	Maybe	Maybe	No
Axial Dispersion	No	No	No
Heterogeneity	Yes	Maybe	Yes
Density Variations	No	No	No

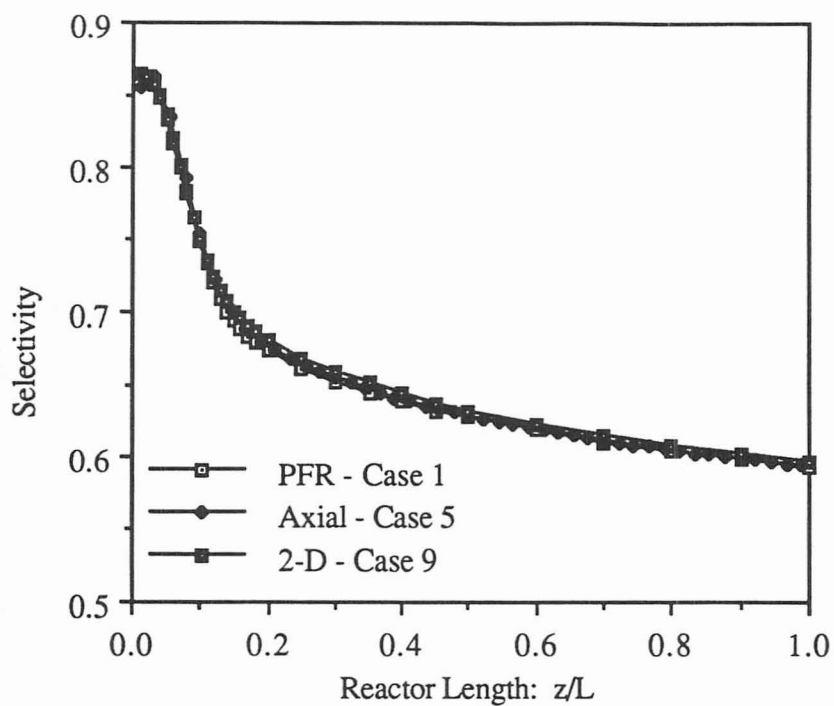


Figure 8.1: Selectivity for the Maleic Anhydride Reactor Comparison

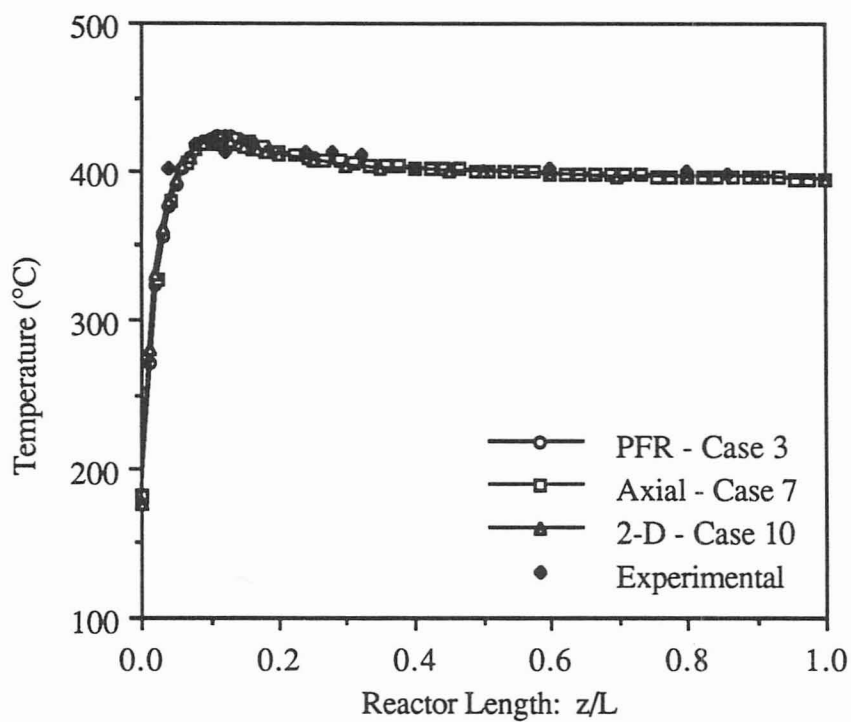


Figure 8.2: Temperature Profiles for the Maleic Anhydride Reactor Comparison. Experimental Data from Sharma, *et al.* (1991).

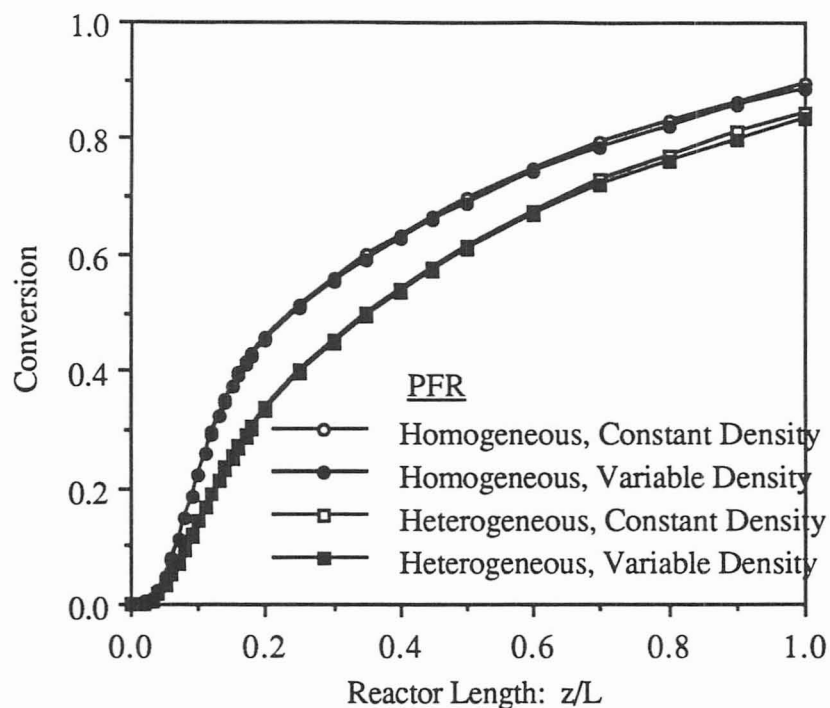


Figure 8.3: Comparison of Conversion for Various Effects in the Maleic Anhydride Reactor. Simulations 1, 2, 3, and 4.

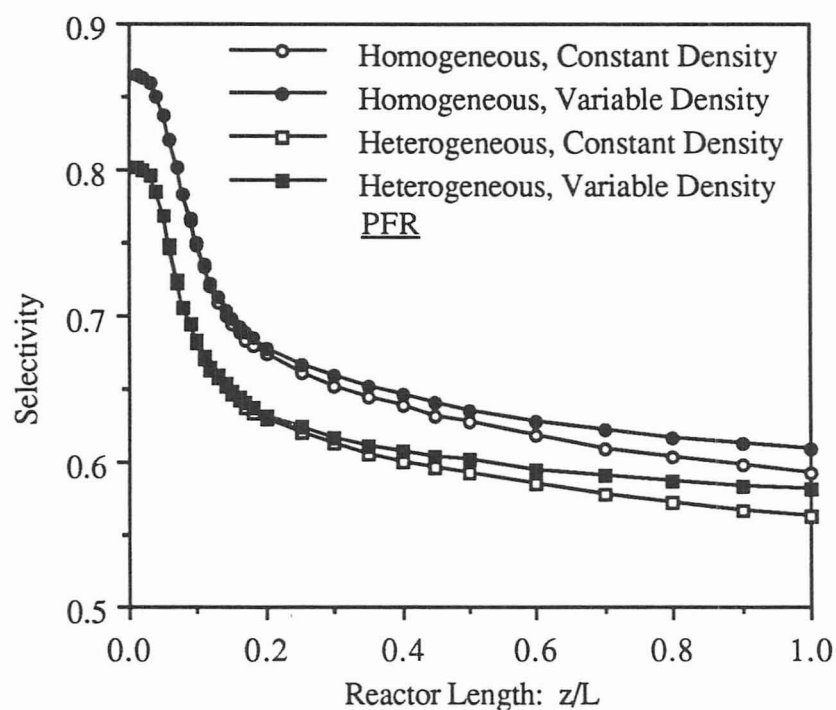


Figure 8.4: Selectivity Comparison for Various Effects in the Maleic Anhydride Reactor. Simulations 1, 2, 3, and 4.

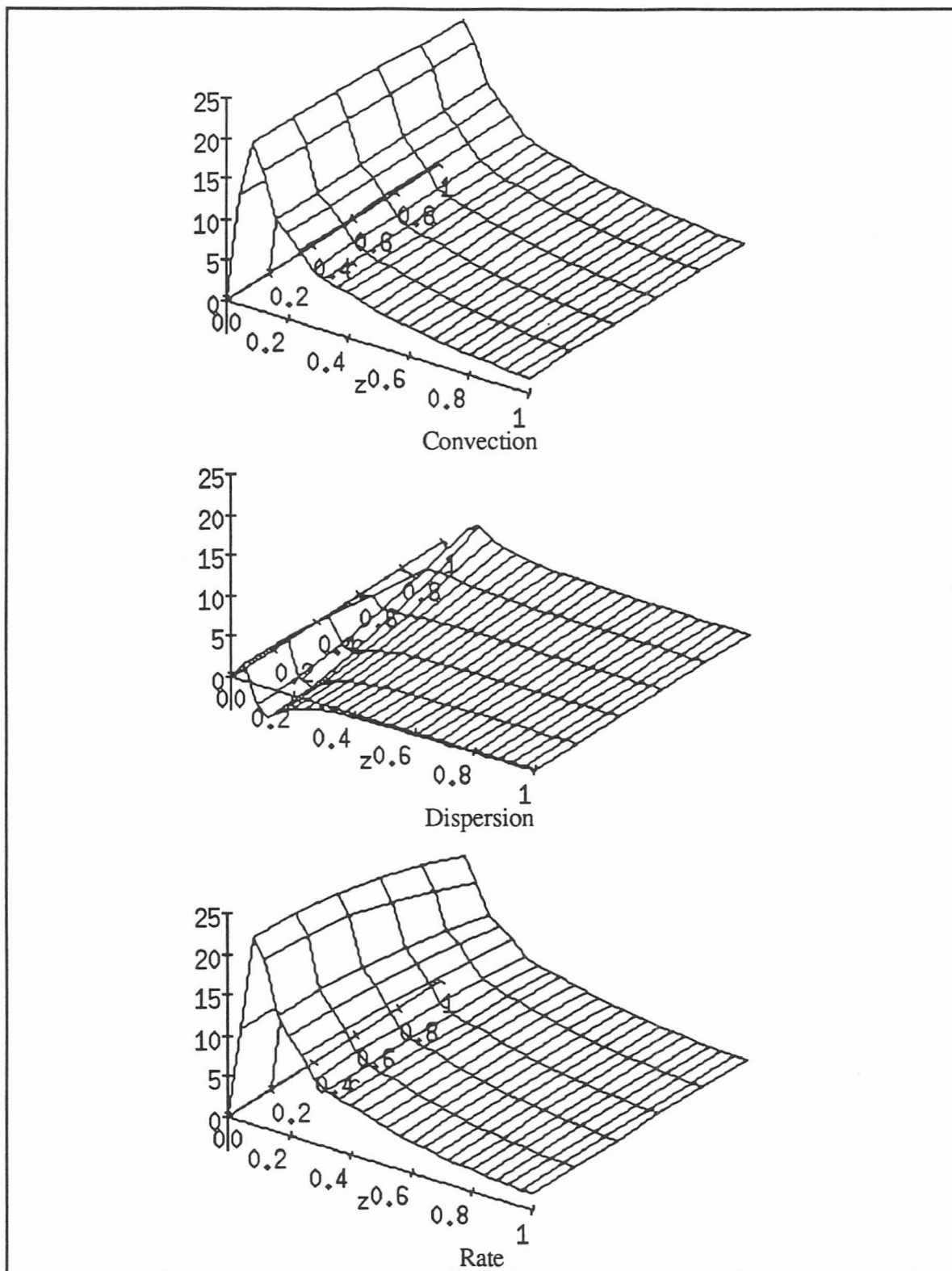


Figure 8.5: Convection, Dispersion, and Rate Terms for the Maleic Anhydride Mass Balance

Chapter 9. Conclusions and Recommendations

The goal of this thesis has been to describe the Chemical Reactor Design Tool and to demonstrate some of its uses. The models that CRDT uses allow the design of a reactor with the possibility of including many different phenomena. These models take into account many effects that are often neglected in order to simplify the model so it can be solved analytically or with simple software packages. These effects include density variations, pressure drop, velocity variations, heterogeneous effects, multiple reactions, and heating and cooling at the wall.

The user has a choice of methods to solve the model. Comparison of the different methods offers a way for checking to see if the solution is accurate. If two methods give differing results, the user can choose more grid points in the domain or smaller tolerances or time steps for the integration routine. It also teaches the user about the different methods and can demonstrate why one method may be better in certain circumstance than another method. The methods are very robust. Concentrations and temperatures within the bounds of the reaction system are given to the non-linear algebraic equations solver as an initial guess as an attempt to be within the radius of convergence. If this initial guess is not within the radius of convergence for the Newton-Raphson method, a more robust homotopy method is applied. A large range for the number of grid points is provided to the user. The user can choose either an explicit or implicit integration routine, whichever is best suited for their particular problem.

CRDT is an effective teaching and design tool. The ability to use a computer to do the modeling is a great advantage. This allows the use of complicated models. The solution time saved also allows the user to compare many different models. The graphical output visually demonstrates to the student what affect including a certain phenomenon has on the solution. Reactor design principles are communicated excellently with the ability to view the results graphically. Some simplifications that are required so the student can solve

the problem can be time consuming and confusing. These need not be made with CRDT. The effects of these simplifications can be studied with CRDT. For example, side reactions need not be neglected since they are as easy to include as the main reaction. The student can solve the problem again without the side reactions to study the effect of the simplification.

Design decisions can also be made with CRDT. The effects of catalyst packing are numerous. Just the size of the catalyst can effect heterogeneity, pressure drop, dispersion, and heat transfer. If there are changes in any of these phenomena, there is a potential change in the product yield. All these effects can be easily analyzed with CRDT. *A priori* criterion can be used to estimate the importance of certain effects, but the predictions are not always accurate.

The criteria used in this thesis are better than many of the criteria in literature. The criterion developed predict changes in concentrations. Many of the literature criteria predict changes in reaction rates. What is important to know is if the phenomenon will change product yield, not reaction rates. Also, the simplicity of these criteria makes them easy to apply.

It is not possible to model every reactor with CRDT. The two-dimensional, gas-phase reactors with variable density tested produce non-physical results. This model treats concentrations and temperature as functions of both radius and length, but pressure as only a function of reactor length. If concentration and temperature vary radially, then pressure should also. Therefore, the next logical step for this project is to develop a better model for the two-dimensional reactor that includes a two-dimensional momentum balance.

Other recommendations for improvements include adding the finite element method for the solution of the PFR with axial diffusion model. This would allow the user to see the how important the treatment of the boundary conditions is in a numerical method by comparing the finite difference and finite element methods. Another important addition to

the PFR with axial diffusion problem is to back up the Newton-Raphson method with the homotopy method. Also, the homotopy method could be improved by ensuring the jacobian will not become singular prior to decomposition.

List of References

- Bird, R.B., Stewart, W.E. and E.N. Lightfoot, *Transport Phenomena*, John Wiley & Sons, New York, (1960).
- Brankin, R.W., Gladwell, I., and L.F. Shampine, 'RKSUITE', *Softreport 92-S1*, Dept. of Math, SMU, Dallas, (1992).
- Edgar, T.F. and D.M. Himmelblau, *Optimization of Chemical Processes*, McGraw-Hill, New York, (1988).
- Finlayson B.A., Rosendall, B.M., Godfrey, G., and S. Lee, *Chemical Reactor Design Tool, Student Manual and Textbook Supplement*, Dept. of Chemical Engineering, University of Washington, Seattle, (1994).
- Finlayson B.A., Rosendall, B.M., Godfrey, G., and S. Lee, *Chemical Reactor Design Tool, Instructor's Reference Manual*, Dept. of Chemical Engineering, University of Washington, Seattle, (1994).
- Finlayson, B.A., *Numerical Methods for Problems with Moving Fronts*, Ravenna Park Publishing, Seattle, 1992.
- Finlayson, B.A., *Nonlinear Analysis in Chemical Engineering*, McGraw-Hill, New York, (1980).
- Finlayson, B.A., 'Orthogonal Collocation in Chemical Reaction Engineering', *Cat. Rev. Sci. Eng.*, 10, 69 (1974).
- Fogler, H.S., *Elements of Chemical Reaction Engineering*, Prentice-Hall, Englewood Cliffs, (1986).
- Froment, G.F., and K.B. Bischoff, *Chemical Reactor Analysis and Design*, John Wiley & Sons, New York (1990).
- Froment, G.F., 'Fixed Bed Catalytic Reactors', *Ind. Eng. Chem.*, 59, 18 (1967).
- Gavalas, G.R. *Nonlinear Differential Equations of Chemically Reacting Systems*, Springer Tracts in Natural Philosophy, Springer-Verlag, New York, (1968)
- Hill, C.J., *An Introduction to Chemical Engineering Kinetics and Reactor Design*, John Wiley & Sons, New York, (1977).
- Hindmarsh, A.C., *ODEPACK, A Systematized Collection of ODE Solvers*, in *Scientific Computing*, R.S. Stepleman, et al. (Eds.), North-Holland, Amsterdam, 55 (1983)
- Levenspiel, O. and K.B. Bischoff, *Advan. Chem. Eng. Progr.* 46, 614 (1950).
- Mears, D. E., 'Diagnostic Criteria for Heat Transport Limitations in Fixed Bed Reactors', *J. Catal.* 20, 127-131, (1971).
- Press, W.H., Flannery, B.P., Teukolsky, S.A. and W.T. Vetterling, *Numerical Recipes*, Cambridge University Press, (1989).

- Seader, J.D., 'Computer Modeling of Chemical Processes', *AIChE Monogr. Ser.*, No. 15, 81, 26 (1985)
- Schuler, R.W., Stallings, V.P., and J.M. Smith, 'Heat and Mass Transfer in Fixed-Bed Reactors', *Chem. Eng. Progr. Symp. Ser.*, No. 4, 48, 19 (1954)
- Sharma, R.K., Cresswell, D.L., and E.J. Newson, 'Kinetics and Fixed-Bed Reactor Modeling of Butane Oxidation to Maleic Anhydride', *AIChE J.*, 37(1), 39 (1991).
- Yagi, S., Kunii, D., and N. Wakao, 'Studies on Axial Effective Thermal Conductivities in Packed Beds', *AIChE J.*, 6(4), 543 (1960).
- Young, L.C. and B.A. Finlayson, 'Axial Dispersion in Nonisothermal Packed Bed Chemical Reactors', *Ind. Eng. Chem. Fundam.*, 12(4), 412 (1973).

Appendix A. Nomenclature

a = geometry factor: 1 = planar, 2 = cylindrical, 3 = spherical.

a = Catalyst surface area/bed volume, m^{-1} .

A_c = Cross sectional area of reactor, m^2 .

A_w = Area for heat transfer, m^2 .

Bi = Biot number, $h_w/(\lambda_{er}R_t)$.

C_j = Concentration of species j , $kmol/m^3$.

C_{j0} = Inlet concentration of species j , $kmol/m^3$.

C_T = Total concentration, $kmol/m^3$.

C_{T0} = Inlet total concentration, $kmol/m^3$.

$C_{s,j}$ = Surface concentration of species j , $kmol/m^3$.

C_{pj} = Specific heat of species j , $kJ/(kmolK)$.

C_{pj0} = Inital/inlet specific heat of species j , $kJ/(kmolK)$.

d_p = Particle diameter, m .

d_t = Reactor diameter, m .

Da_I = Damköhler number for mass, $\rho_B R_0 V / F_{tot}$.

Da_{III} = Damköhler number for heat, $\rho_B R_0 V (-\Delta H_{rxn,1}) / ([\sum F_j C_{pj}]_0 T_{ref})$.

D_e = Effective diffusivity, $m^2/mcat.s$.

$D_{ea,j}$ = Effective axial dispersion coefficient for species j , m^2/s .

$D_{er,j}$ = Effective radial dispersion coefficient for species j , m^2/s .

E = Activation energy, $kJ/kmol$.

F_j = Molar flow rate of species j , $kmol/s$.

F_{j0} = Initial/inlet molar flow rate of species j , $kmol/s$.

F_T = Total molar flow rate, $kmol/s$.

F_{T0} = Initial/inlet total molar flow rate, $kmol/s$.

G = Mass flux, $\text{kg}/(\text{m}^2\text{s})$.

h_p = Particle heat transfer coefficient, $\text{kJ}/(\text{m}^2\text{sK})$.

h_w = Wall heat transfer coefficient, $\text{kJ}/(\text{m}^2\text{sK})$.

$\Delta H_{\text{rxn},i}$ = Heat of reaction for reaction i , kJ/kmol .

$k(T)$ = First-order rate constant, s^{-1} .

k_e = effective thermal conductivity in a solid particle, $\text{kJ}/(\text{m}\cdot\text{s}\cdot\text{K})$.

k_m = Particle mass transfer coefficient, m/s .

k_w = Particle mass transfer coefficient, m/s .

L = Reactor Length, m .

M = Total number of reactions.

MW_j = Molecular weight of species j , kg/kmol .

N = Total number of components.

N_j = Number of moles of species j , kmol .

N_{j0} = Initial number of moles of species j , kmol .

N_T = Total number of moles, kmol .

N_{T0} = Initial total number of moles, kmol .

P = Pressure, Pa .

P_0 = Initial/inlet pressure, Pa .

P_j = Partial pressure of species j , Pa .

$Pe_{\text{ma},j}$ = Axial mass Peclet number, $u_0 d_p / (\epsilon D_{\text{ea},j})$.

$Pe_{\text{mr},j}$ = Radial mass Peclet number, $u_0 d_p / (\epsilon D_{\text{er},j})$.

$Pe_{\text{mL},j}$ = Axial mass Peclet number, $u_0 L / (\epsilon D_{\text{ea},j})$.

$Pe_{\text{h,L}}$ = Axial heat Peclet number, $u_0 L [\sum F_j C_{p,j}]_0 / \lambda_{\text{ea}}$.

$Pe_{\text{h,r}}$ = Radial heat Peclet number, $u_0 d_p [\sum F_j C_{p,j}]_0 / \lambda_{\text{er}}$.

r' = Dimensionless radius.

r_i = Rate expression for reaction i , $\text{kgcat}/(\text{m}^3\text{s})$.

R = Reactor radius, m.

R_g = Gas constant, kJ/kmolK.

R_j = Reaction rate of species j, kgcat/(m³s).

R_t = Radius of reactor, m.

Re = Particle Reynolds' number, $\rho u_0 d_p / \mu$.

S = Selectivity.

St = Stanton number, $UL / (d_t G C_p)$.

t = time, s.

T = Temperature, K.

T_0 = Initial/inlet temperature, K.

T_s = Surface temperature, K.

T_w = Wall temperature, K.

u = Velocity, m/s.

u_0 = Initial/inlet velocity, m/s.

U = Overall heat transfer coefficient, kJ/(m²sK).

V_R = Reactor volume, m³.

V_{R0} = Initial reactor volume, m³.

X = $C_{SO_2} / C_{SO_2,0}$.

y_{a0} = Mole fraction of limiting reactant.

y_j = Mole fraction of species j.

z = Axial distance, m.

Greek symbols

ϵ = Void fraction in packed bed.

ϵ_a = Mole change parameter.

δ = Increase in the total number of moles per mole limiting reactant reacted.

$\gamma_w = E/R_g T_w$.

ϕ = Thiele modulus.

η = Effectiveness factor.

λ_{ea} = Effective axial dispersion thermal conductivity, kJ/(msK).

λ_{er} = Effective radial dispersion thermal conductivity, kJ/(msK).

μ = viscosity, kg m/s.

v_{ji} = Stoichiometric coefficient of species j in reaction i.

v_j = Stoichiometric coefficient of species j.

v_a = Stoichiometric coefficient of limiting reactant.

ρ = Density, kg/m³.

ρ_0 = Initial/inlet density, kg/m³.

ρ_B = Bulk catalyst density, kgcat/m³.

v = Volumetric flow rate, m³/s

Appendix B: FORTRAN Rate Subroutines

B.1. Sulfur Trioxide Reactor

```
      subroutine rate(kon,c,ra,eta,t,rt,etat)
      double precision c(21),eta(21),ra(21),t,rt,etat,rkeq,rk1,rk2,r1,to,rtop,rbot,x,yao
      go to (5,20), kon
5      return
      c
      c      set effectiveness factors to 1.0
      c
20     do i = 1,4
           eta(i) = 1.0
        enddo
        etat = 1.0

      c
      c      define parameters
      c
      to = 673.0
      yao = 0.065
      rkeq = exp(-11.02 + 11570.0/(t*to))
      rk1 = exp(-14.960 + 11070.0/(t*to))
      rk2 = exp(-1.3310 + 2331.0/(t*to))

      c
      c      define x
      c
      x = c(1)/yao

      c
      c      calculate rate expression
      c
      rtop = x*sqrt(1.0 - 0.166*(1.0-x))-2.2*(1.0-x)/rkeq
      rbot = (rk1 + rk2*(1.0-x))**2
      r1 = rtop/rbot/3600.0

      c
      c      calculate species rates
      c      1 - sulfur dioxide
      c      2 - oxygen
      c      3 - sulfur trioxide
      c      4 - nitrogen
      c
      ra(1) = -r1
      ra(2) = -0.50*r1
      ra(3) = r1
      ra(4) = 0.0

      c
      c      calculate rate for energy balance
      c
      rt = r1

      c
      return
      end
```

B.2. Phthalic Anhydride Reactor

```

subroutine rate(kon,c,ra,eta,t,rt,etat)
double precision c(21),eta(21),ra(21),par(8),p(20)
double precision t,rt,etat,rk1,rk2,rk3,r1,r2,r3,to
integer kon,i
common /tosave/ par
go to (5,20), kon
5  continue
   return
20  continue

```

c set reference temperature

```
to = 628.0
```

c set effectiveness factors to 1

```
do i = 1,6
    eta(i) = 1.
enddo
etat = 1.

```

c convert to partial pressures

```
call partpres(c,p)
```

c calculate rate constants

```
rk1 = exp(19.837-13588.0/(t*to))
rk2 = exp(20.86-15803.0/(t*to))
rk3 = exp(18.97-14394.0/(t*to))

```

c calculate rate expressions

```
r1 = rk1*p(1)*p(5)/3600.0
r2 = rk2*p(2)*p(5)/3600.0
r3 = rk3*p(1)*p(5)/3600.0

```

c calculate species rates

```
ra(1) = -r1 - r3
ra(2) = r1 - r2
ra(3) = 3.0*r1 + 2.0*r2 + 5.0*r3
ra(4) = 8.0*r2 + 8.0*r3
ra(5) = -3.0*r1 - 7.5*r2 - 10.5*r3
ra(6) = 0.0
rt = 1.0*r1 + 2.552*r2 + 3.552*r3
return
end

```

B.3. Maleic Anhydride Reactor

```

subroutine rate(kon,c,ra,eta,t,rt,etat)
double precision c(21), eta(21), ra(21), par(8), p(20)
double precision t, rt, etat, ts, ps, rk1, rk2, rk3, r1, r2, r3, etar1, etar2, etar3, zf
integer kon, i
common /zrate/ zf
common /tosave/ ts,ps
go to (5,20), kon
5  return
20 continue

c      1 - n-butane
c      2 - maleic anhydride
c      3 - carbon monoxide
c      4 - water
c      5 - carbon dioxide
c      6 - oxygen
c      7 - nitrogen

c set constants

      ts = 663.0
      ps = 1.65

c determine effectiveness factor

      if(zf.ge.0.8) then
          etar1 = 0.9
          etar2 = 1.02
          etar3 = .92
      elseif(zf.ge.0.4) then
          etar1 = 0.89
          etar2 = 1.06
          etar3 = 0.95
      elseif(zf.ge.0.2) then
          etar1 = .82
          etar2 = 1.15
          etar3 = 0.95
      elseif(zf.ge.0.12) then
          etar1 = .72
          etar2 = 1.38
          etar3 = 0.94
      elseif(zf.ge.0.08) then
          etar1 = .66
          etar2 = 1.72
          etar3 = .95
      else
          etar1 = .62
          etar2 = 2.8
          etar3 = .98
      endif
endif

```

```

do i = 1,7
    eta(i) = 1.
enddo
etat = 1.

c convert to partial pressures

    call partpres(c,p)

c calculate rate constants

    rk1 = 0.96e-6*exp(93100.0/8.3140/673.0*(1.0-673.0/(t*ts)))
    rk2 = 0.29e-5*exp(155000.0/8.3140/673.0*(1.0-673.0/(t*ts)))
    rk3 = 0.15e-6*exp(93100.0/8.3140/673.0*(1.0-673.0/(t*ts)))

    if (p(1).le.0) then

c protect from crashing

        r1 = 0.0
        r2 = etar2*rk2*ps*p(2)/(1.0+310.0*ps*p(2))**2
        r3 = 0.0

c calculate rate expressions

        else
            r1 = etar1*rk1*(ps*p(1))**0.54/(1.0+310.0*ps*p(2))
            r2 = etar2*rk2*ps*p(2)/(1.0+310.0*ps*p(2))**2
            r3 = etar3*rk3*(ps*p(1))**0.54
        endif

c calculate reaction rates

        ra(1) = -r1 - r3
        ra(2) = r1 - r2
        ra(3) = 4.0*r2 + 2.0*r3
        ra(4) = 4.0*r1 + r2 + 5.0*r3
        ra(5) = 2.0*r3
        ra(6) = -3.50*r1 - r2 - 5.50*r3
        ra(7) = 0.0

        rt = 1.0*r1 + 0.23*r2 + 1.69*r3

    return
end

```